Meteoritics & Planetary Science 36, 301–317 (2001)
Available online at http://www.uark.edu/meteor

Cosmic-ray exposure history of two Frontier Mountain H-chondrite showers from spallation and neutron-capture products

K. C. WELTEN[1], K. NISHIIZUMI[1], J. MASARIK[1 *], M. W. CAFFEE[2], A. J. T. JULL[3], S. E. KLANDRUD[3] AND R. WIELER[4]

[1]Space Sciences Laboratory, University of California, Berkeley, California 94720-7450, USA
[2]Geosciences and Environmental Technology Division, Lawrence Livermore National Laboratory, Livermore, California 94550, USA
[3]NSF Arizona AMS Laboratory, University of Arizona, P.O. Box 210081, Tucson, Arizona 85721, USA
[4]ETH Zürich, Isotope Geology and Mineral Resources, NO C61, CH-8092 Zürich, Switzerland
[†]Present address: Department of Nuclear Physics, Komensky University, Bratislava, Slovakia
*Correspondence author's e-mail address: kcwelten@uclink4.berkeley.edu

(Received 2000 May 25; accepted in revised form 2000 October 25)

Abstract–We measured the concentrations of ^{10}Be, ^{26}Al, ^{36}Cl, ^{41}Ca and ^{14}C in the metal and/or stone fractions of 27 Antarctic chondrites from Frontier Mountain (FRO), including two large H-chondrite showers. To estimate the pre-atmospheric size of the two showers, we determined the contribution of neutron-capture produced ^{36}Cl (half-life = 3.01×10^5 years) and ^{41}Ca (1.04×10^5 years) in the stone fraction. The measured activities of neutron-capture ^{36}Cl and ^{41}Ca, as well as spallation produced ^{10}Be and ^{26}Al, were compared with Monte Carlo-based model calculations. The largest shower, FRO 90174, includes eight fragments with an average terrestrial age of $(100 \pm 30) \times 10^3$ years; the neutron-capture saturation activities extend to 27 dpm/kg stone for ^{36}Cl and 19 dpm/kg stone for ^{41}Ca. The concentrations of spallation produced ^{10}Be, ^{26}Al and ^{36}Cl constrain the radius (R) to 80–100 cm, while the neutron-capture ^{41}Ca activities indicate that the samples originated from the outer 25 cm. With a pre-atmospheric radius of 80–100 cm, FRO 90174 is among the largest of the Antarctic stony meteorites. The large pre-atmospheric size supports our hypothesis that at least 50 of the ~150 classified H5/H6-chondrites from the Frontier Mountain stranding area belong to this single fall; this hypothesis does not entirely account for the high H/L ratio at Frontier Mountain. The smaller shower, FRO 90001, includes four fragments with an average terrestrial age of $(40 \pm 10) \times 10^3$ years; they contain small contributions of neutron-capture ^{36}Cl, but no excess of ^{41}Ca. FRO 90001 experienced a complex exposure history with high shielding conditions in the first stage ($150 < R < 300$ cm) and much lower shielding in the second stage ($R < 30$ cm), the latter starting ~1.0 million years (Ma) ago. Based on the measured ^{10}Be/^{21}Ne and ^{26}Al/^{21}Ne ratios, the cosmic-ray exposure ages of the two showers are 7.2 ± 0.5 Ma for FRO 90174 and 8 ± 1 Ma for FRO 90001. These ages coincide with the well-established H-chondrite peak and corroborate the observation that the exposure age distribution of FRO H-chondrites is similar to that of non-Antarctic falls. In addition, we found that corrections for neutron-capture ^{36}Ar (from decay of ^{36}Cl) result in concordant ^{21}Ne and ^{38}Ar exposure ages.

INTRODUCTION

Most cosmogenic nuclides in meteorites are produced by spallation reactions, but in large objects, such as Allende, Chico, Jilin, Torino and Knyahinya, thermal neutron-capture also plays a role (Cressy, 1972; Klein *et al.*, 1991; Nishiizumi *et al.*, 1991a; Reedy *et al.*, 1993; Bogard *et al.*, 1995). Radionuclides produced by neutron-capture include ^{59}Ni (half-life = 7.6×10^4 years) and ^{60}Co (5.27 years) in the metal phase, and ^{36}Cl (3.01×10^5 years) and ^{41}Ca (1.04×10^5 years) in the silicate phase. The concentrations of these neutron-capture products provide valuable information about the pre-atmospheric size of a meteorite and the shielding depth of a sample within the meteoroid.

Antarctic meteorites are not the most likely objects to search for neutron-capture products: their recovered masses are on average ~100 times smaller than the masses of non-Antarctic meteorites. Nevertheless, it has been suggested that the Antarctic meteorite collection contains many unrecognized showers (Huss, 1991), some of which may have been derived from large objects. We found that up to 12 out of 26 Frontier Mountain (FRO) H-chondrites belong to two large showers based on cosmogenic nuclide concentrations (Welten *et al.*, 1999a). The largest shower (FRO 90174) includes at least

seven small fragments (4–20 g) with $^{22}Ne/^{21}Ne$ ratios of 1.07–1.10 in bulk samples and low concentrations of ^{10}Be (half-life = 1.5×10^6 years), ^{26}Al (7.05×10^5 years) and ^{36}Cl in the metal phase (Welten *et al*., 1999a). On the basis of the $^{36}Cl/^{10}Be$ versus ^{10}Be correlation (Nishiizumi *et al*., 1997a), we determined a terrestrial age of 100 ± 25 ka for the FRO 90174 shower, which corresponds to ^{36}Cl saturation values of 15–21 dpm/kg metal. These values are significantly lower than those measured in Knyahinya (20–22 dpm/kg) (Reedy *et al*., 1993), suggesting that the fragments of the FRO 90174 shower were derived from an object larger than 45 cm in radius and thus are likely to contain neutron-capture ^{36}Cl and ^{41}Ca in the stony phase.

The second shower (FRO 90001) contains four fragments with $^{22}Ne/^{21}Ne$ ratios of 1.05–1.08. The lower $^{22}Ne/^{21}Ne$ ratios suggest higher shielding than observed in the FRO 90174 shower. However, the radionuclide concentrations indicate lower shielding conditions during the recent exposure, which implies a complex exposure history for the FRO 90001 shower. Multi-nuclide studies can in many instances detect a complex exposure history, but despite the increase of multi-nuclide studies, well-constrained complex exposure histories have only been identified for 10–20 ordinary chondrites (*e.g.*, Vogt *et al*., 1993; Herzog *et al*., 1997). Complex exposure histories provide additional constraints on orbital dynamics models, which simulate the transport of meteoroids from the asteroid belt to Earth. These two-stage scenarios are especially significant: recent developments in orbital mechanics models indicate the presence of a mechanism that transports meteoroids slowly from the main belt to the resonances, after which they are delivered, within a few million years, into Earth-crossing orbits (*e.g.*, Morbidelli and Gladman, 1998; Hartmann *et al*., 1999; Bottke *et al*., 2000).

We measured concentrations of ^{10}Be, ^{26}Al, ^{36}Cl and ^{41}Ca in the metal and silicate fractions of the two H-chondrite showers. In addition, ^{14}C was measured in the stone fraction of the FRO 90001 shower and other samples with high ^{36}Cl concentrations in order to constrain their terrestrial age. Our primary objective is to determine the contribution of neutron-capture produced ^{36}Cl and ^{41}Ca in the silicate fraction as well as spallation-produced ^{10}Be and ^{26}Al in metal and stone fractions, and compare these with theoretical production rate calculations to estimate the pre-atmospheric size of the two showers and constrain their exposure history. Once the pre-atmospheric size is known we use the semi-empirical model of Graf *et al*. (1990) to re-evaluate the cosmic-ray exposure ages of these two objects. Initial work was presented earlier (Welten *et al*., 1999b).

EXPERIMENTAL

Meteorite Samples

We selected the four members of the FRO 90001 shower and all possible members of the FRO 90174 shower, discussed by Welten *et al*. (1999a). We consider FRO 90012 to be part of the FRO 90174 shower, since its radionuclide concentrations are very similar to those of the shower and quite different from all other samples. FRO 90012 was initially not recognized as part of the shower, since it contains large quantities of solar noble gases, as evidenced by its $^{20}Ne/^{22}Ne$ ratio of 9.1. In fact, FRO 90174 itself also shows an elevated $^{20}Ne/^{22}Ne$ ratio of 1.83, whereas all other members of the shower have $^{20}Ne/^{22}Ne$ ratios near the cosmogenic value of 0.83. Heterogeneous siting of solar gases within gas-rich samples is common (König *et al*., 1961). A possible explanation is that meteorites incorporate varying amounts of solar-gas-bearing dust. Hence, it is well conceivable that FRO 90012 and to a lesser extent FRO 90174 are the only analysed samples of the FRO 90174 shower that contain such former asteroidal dust. Although the sample was not identified as a breccia, this structure is easily overlooked in small specimens, such as the members of the FRO 90174 shower, which are all less than 20 g. Finally, cosmogenic noble gases are consistent with the pairing assignment of FRO 90012; however, because more than 50% of all H-chondrites show exposure ages between 4–10 Ma, as do FRO 90012 and all unambiguous members of the FRO 90174 shower, the cosmogenic noble gases alone are not equivocal. In addition to the two showers, we measured all other FRO H-chondrites and one L-chondrite discussed in Welten *et al*. (1999a).

Radionuclide Analyses

Bulk samples of 1–2 g were crushed in an agate mortar and separated into a magnetic and a non-magnetic ("silicate") fraction. The magnetic fraction was cleaned several times in an ultrasonic bath with 0.2 N HCl and once with concentrated HF to dissolve attached troilite and silicates. In this way, we obtained clean metal with less than 0.2% silicates. The measurements of ^{10}Be, ^{26}Al, ^{36}Cl in the metal fraction were described in a previous study (Welten *et al*., 1999a). In this work we separated Ca from the remaining solution by cation exchange chromatography. The Ca was first precipitated as Ca oxalate, then dissolved in 0.5N HCl and precipitated as CaF_2 by HF. The CaF_2 was washed with dilute HF and Milli-Q water, dried in a furnace at 500 °C, and then mixed with Ag powder (2:1 wt/wt) and loaded into Al target holders. The silicate fraction was dissolved with HF/HNO_3 mixture along with Be and Cl carrier. After Cl was isolated as AgCl, an aliquot was taken for chemical analysis by atomic absorption spectroscopy (AAS). Al and Ca carriers were added. Be and Al were separated by anion exchange chromatography, acetylacetone solvent extraction, and cation exchange chromatography. Ca was separated from the aqueous fraction of the extraction step and converted to CaF_2 as described above. The Be and Al fractions were further purified and converted to BeO and Al_2O_3, respectively, for AMS measurements.

The ^{10}Be, ^{26}Al, ^{36}Cl and ^{41}Ca concentrations were determined using the Lawrence Livermore National Laboratory tandem accelerator (Davis *et al*., 1990). The measured ^{10}Be/^{9}Be ratios ranged from 5×10^{-12} to 8×10^{-12}, the ^{26}Al/^{27}Al ratios from 7×10^{-12} to 1.4×10^{-11}, the ^{36}Cl/Cl ratios from 8×10^{-13} to 8×10^{-12}. The ^{41}Ca/Ca ratios range from 1×10^{-13} to 2×10^{-12} for the silicate fraction and from 2×10^{-13} to 4×10^{-12} for the metal fraction. After making corrections for isobaric interferences (^{10}B for ^{10}Be and ^{36}S for ^{36}Cl), and for chemical blanks (3×10^{-14} for ^{10}Be/Be, $\sim 2 \times 10^{-15}$ for ^{26}Al/Al, $\sim 3 \times 10^{-15}$ for ^{36}Cl/Cl, and $\sim 5 \times 10^{-14}$ for ^{41}Ca/Ca), the measured ratios were normalized to an ICN ^{10}Be standard (ICN Radiochemicals), NBS (National Bureau of Standards, present National Institute of Standards and Technology) ^{26}Al and ^{36}Cl standards and new ^{41}Ca standards. All AMS standards were prepared by one of the authors (Nishiizumi *et al*., 1984, 2000; Sharma *et al*., 1990). In addition, for samples with ^{36}Cl/^{10}Be terrestrial ages $\leq$60 ka, we also measured ^{14}C in the silicate fraction to determine the terrestrial age more accurately. The ^{14}C measurements were performed at the University of Arizona NSF-AMS facility (Jull *et al*., 1998).

Model Calculations

We used the Los Alamos High Energy Transport (LAHET) Code System (LCS) to calculate the primary and secondary particle fluxes in cosmic-ray irradiated H-chondrites with radii ranging from 4 to 200 cm (Masarik and Reedy, 1994). The transport of high-energy particles is done with the LAHET code (Prael and Lichtenstein, 1989), whereas neutrons with energies below a cut-off energy of 15 MeV are further transported to thermal energies (~0.02 eV) by the Monte Carlo N-Particle (MCNP) code (Briesmeister, 1993). Using the fluxes of high-energy particles, we calculated the production rates of ^{36}Cl in the metal phase and of ^{10}Be and ^{26}Al in both the metal and stone fractions. For the production of ^{10}Be we included reactions on O, Mg, Al, Si, Fe and Ni, since other target elements contribute less than 1% of the total ^{10}Be production. For the production of ^{26}Al we also included production rates from S. The model calculations were previously shown to agree within about 10% with the measured concentrations in the metal and stone fraction of the Knyahinya L-chondrite (Reedy *et al*., 1993). Based on the calculated thermal neutron fluxes and thermal neutron-capture cross sections of 44 barn for ^{35}Cl and 0.43 barn for ^{40}Ca (Mughabghab *et al*., 1981), we also calculated the (n,γ) production rates of ^{36}Cl and ^{41}Ca in the silicate phase. For the calculations we assumed average H-chondrite abundances of 80 ppm Cl and 1.25% Ca (Mason, 1979). In order to make accurate corrections for the spallation component of ^{36}Cl, production rates of ^{36}Cl from Ca and K relative to that of ^{36}Cl from Fe were calculated as a function of shielding conditions.

RESULTS AND DISCUSSION

Elemental Concentrations

Concentrations of Al, K, Ca, Fe and Ni, measured by AAS of small aliquots of the dissolved stone fraction, are shown in Table 1. The measured Fe and Ni concentrations in the stone fraction are significantly higher than average literature values of 13.5 ± 0.5 wt% Fe (Welten, 1999; derived from FeO and FeS analyses of Jarosewich, 1990) and 0.05 ± 0.02 wt% Ni (Rambaldi *et al*., 1978) for H-chondrite falls. These high Fe and Ni concentrations indicate that the stone fraction of most FRO samples contains significant amounts of oxidized metal due to terrestrial weathering (Welten and Nishiizumi, 2000).

TABLE 1. Elemental concentrations and amount of oxidized metal in the stone fraction of Frontier Mountain H chondrites.

FRO	Al*	K*	Ca*	Fe*	Ni*	$f(M_{OX})^{\dagger}$
FRO 90001 shower						
90001	1.22	0.091	1.24	17.2	0.80	0.087
90050	1.28	0.085	1.19	18.8	1.02	0.122
90073	1.21	0.093	1.22	17.5	0.73	0.092
90152	1.37	0.091	1.25	17.4	0.75	0.090
FRO 90174 shower						
8403	1.27	0.095	1.32	17.7	0.87	0.099
90012	1.27	0.091	1.19	18.2	1.02	0.111
90087	1.31	0.092	1.26	17.7	1.05	0.101
90107	1.22	0.090	1.26	16.9	1.13	0.088
90174	1.34	0.092	1.27	16.8	0.84	0.080
90203	1.26	0.086	1.23	18.2	0.90	0.108
90204	1.15	0.095	1.32	18.4	0.92	0.111
90207	1.21	0.091	1.36	16.9	0.84	0.081
90211	1.19	0.090	1.24	17.2	0.90	0.088
Other FRO meteorites						
90002‡	1.41	0.100	1.43	15.1	0.39	0.038
90043‡	1.40	0.102	1.43	14.6	0.36	0.027
90069§	1.41	0.094	1.45	14.8	0.57	0.035
90150§	1.33	0.096	1.25	17.2	0.82	0.087
90025#	1.39	0.095	1.38	16.4	0.88	0.072
90151#	1.36	0.097	1.32	14.6	0.50	0.031
90024	1.31	0.085	1.27	17.4	0.95	0.094
90037	1.36	0.094	1.32	17.0	1.06	0.088
90059	1.48	0.101	1.43	14.1	0.38	0.018
90048	1.28	0.108	1.38	16.6	0.67	0.072
90072	1.35	0.103	1.56	15.3	0.38	0.041
90082	1.18	0.090	1.42	19.1	0.87	0.125
90104	1.21	0.088	1.28	17.3	1.00	0.092
8401(L6)	1.41	0.099	1.31	16.1	0.19	0.005

*Elemental concentrations in wt%, uncertainties are 1–2%.
†Amount of oxidized metal in stone fraction.
‡, §, #Possible pairings (Welten *et al.*, 1999a).

Based on equations given in Welten (1999), we calculate that the stone fraction of the FRO samples contains between 0.5 wt% (8401) and 12.5 wt% (90082) of oxidized metal (Table 1). This implies that the concentrations of cosmogenic ^{10}Be and ^{26}Al in the stone fraction were significantly diluted, since the concentrations of ^{10}Be and ^{26}Al in the metal phase are much lower. We will discuss how to make corrections for this dilution effect.

Radionuclide Results

The ^{14}C, ^{10}Be, ^{26}Al, ^{36}Cl and ^{41}Ca results are shown in Table 2 along with previous results of ^{10}Be, ^{26}Al, and ^{36}Cl in the metallic fraction (Welten *et al*., 1999a). The uncertainties include all known AMS errors (1σ) but not the uncertainties of the AMS standards. Assuming an H-chondrite saturation value of 46 ± 10 dpm/kg (Jull *et al*., 1998), the measured ^{14}C concentrations correspond to terrestrial ages ranging from 13 ka to >45 ka, but we will use the ^{14}C-^{10}Be method to calculate shielding-corrected terrestrial ages (Jull *et al*., 2000). The concentrations of ^{10}Be and ^{26}Al in the silicate fraction show relatively tight ranges of 14–20 and 35–65 dpm/kg, respectively, whereas the concentrations of ^{36}Cl and ^{41}Ca in members of the FRO 90174 shower show much wider ranges of 3 to 26 dpm/kg and <1 to 11 dpm/kg, respectively. Figure 1a,b shows that the high ^{36}Cl and ^{41}Ca concentrations found in members of the FRO 90174 shower can not solely be explained by spallation-produced ^{36}Cl and ^{41}Ca, but must be due to significant contributions of neutron-capture ^{36}Cl and ^{41}Ca. This will be discussed in more detail below.

Terrestrial Ages Based on ^{14}C-^{10}Be, ^{41}Ca-^{36}Cl and ^{36}Cl-^{10}Be

^{14}C-^{10}Be–Since both ^{14}C and ^{10}Be in stone meteorites are mainly produced by spallation of oxygen, their production ratio is not only independent of shielding conditions, but also of a meteorite's composition. The shielding independence of the ^{14}C/^{10}Be method was illustrated by a set of samples of the Gold Basin meteorite shower, which show a wide range of shielding conditions (Jull *et al*., 2000). We derived ^{14}C-^{10}Be ages from the ^{14}C and ^{10}Be concentrations in the stone fraction, after applying corrections for undersaturation of the ^{10}Be concentration, based on the exposure ages from Welten *et al*. (1999a). We used an average production rate ratio of 2.65 ± 0.20, derived from Fig. 1 of Jull *et al*. (2000). For ^{14}C concentrations below 1 dpm/kg, we only give minimum terrestrial ages of 30–45 ka, since at these low levels it cannot be excluded that some of the measured ^{14}C is due to terrestrial contamination (Jull *et al*., 1998).

^{36}Cl-^{10}Be–The ^{36}Cl-^{10}Be terrestrial ages of the FRO samples were previously reported in Welten *et al*. (1999a). The ^{36}Cl-^{10}Be method is based on ^{36}Cl and ^{10}Be concentrations in the metal fraction of stone and iron meteorites falls and was applied for iron meteorite finds with terrestrial ages up to ~0.6 Ma (Nishiizumi *et al*., 1997a). In order to apply this method to chondrites, corrections are necessary for the undersaturation of ^{10}Be in case of meteorites with short exposure ages (<10 Ma). In addition, the ^{36}Cl-^{10}Be method may lead to meaningless negative terrestrial ages for meteorites with unrecognized complex exposure histories, as was shown for the FRO 90001 shower and FRO 90104 (Welten *et al*., 1999a).

^{41}Ca-^{36}Cl–Systematic measurements of ^{36}Cl and ^{41}Ca in the metal phase of chondrites and iron meteorites suggested that the ^{41}Ca/^{36}Cl ratio increases slightly as a function of shielding (Nishiizumi and Caffee, 1998). However, additional ^{41}Ca measurements have yielded a constant ratio of 1.06 ± 0.13 over a wide range of shielding conditions (unpubl. data). Due to the short half-lives of ^{36}Cl and ^{41}Ca, their concentrations are independent of the cosmic-ray exposure age, as long as the irradiation lasted more than 1–2 Ma. The measured ^{41}Ca/^{36}Cl ratios in the metal phase are thus a direct measure of the terrestrial age (Table 3). The ^{41}Ca-^{36}Cl terrestrial ages are in good agreement with the shielding-corrected ^{36}Cl-^{10}Be ages and the ^{14}C-^{10}Be ages, except for meteorites with complex exposure histories. Note that also the ^{36}Cl-^{10}Be age of FRO 90024 is much lower than its ^{41}Ca/^{36}Cl age, which supports a complex exposure history, as suggested by Welten *et al*. (1999c).

In the following discussions, the measured activities were corrected to the time of fall using the adopted terrestrial ages of the last column of Table 3. These adopted ages are either the ^{14}C-^{10}Be ages for samples with ^{14}C activities >1 dpm/kg, or the average of the ^{36}Cl-^{10}Be and ^{41}Ca-^{36}Cl ages, while using the minimum ^{14}C ages (where available) as a lower limit.

Pre-Atmospheric Size of FRO 90001 and FRO 90174

In order to estimate the pre-atmospheric size of the two H-chondrite showers, we first compare the saturation activities of ^{10}Be and ^{26}Al in the stone and metal phase to LCS calculations for objects with pre-atmospheric radii of 45–120 cm (Fig. 2a,b). Before comparing the measured values with the model calculations, we have to correct for the dilution of the stone fraction with oxidized metal. Assuming that ^{10}Be and ^{26}Al were retained within the meteorite while the metal was oxidized, the dilution factor (D) can be estimated from the amount of oxidized metal in the stone fraction, fM_{OX} (Table 1), and the stone/metal ratio for ^{10}Be or ^{26}Al (Table 2), using the following equation which was derived from Welten (1999):

$$D = (1 - fM_{OX}) + 0.65 \times \frac{fM_{OX}}{R(sto/met)} \qquad (1)$$

For members of the two showers, the ^{10}Be concentrations were diluted by 7–11%, those of ^{26}Al by 8–12%. The corrected ^{10}Be and ^{26}Al saturation activities for the FRO 90174 shower indicate a pre-atmospheric radius between 60 and 120 cm, although best agreement between measurements and model is obtained for a 80–100 cm radius. For the FRO 90001 shower,

TABLE 2. Concentrations of ^{14}C in stone and ^{10}Be, ^{26}Al, ^{36}Cl and ^{41}Ca in stone and metal fraction of Frontier Mountain H-chondrites.

FRO	^{14}C (stone)	^{10}Be (stone)	^{26}Al (stone)	^{36}Cl (stone)	^{41}Ca (stone)	^{10}Be* (metal)	^{26}Al* (metal)	^{36}Cl* (metal)	^{41}Ca (metal)	$^{41}Ca/^{36}Cl$ (metal)	^{10}Be(sto)/ ^{10}Be(met)†	^{26}Al(sto)/ ^{26}Al(met)†
FRO 90001 shower												
90001	0.96 ± 0.10	17.4 ± 0.2	56.6 ± 1.4	7.7 ± 0.2	3.3 ± 0.4	3.54 ± 0.08	3.06 ± 0.09	21.4 ± 0.2	19.9 ± 1.7	0.93 ± 0.08	5.33 ± 0.13	20.2 ± 0.8
90050	0.22 ± 0.04	16.4 ± 0.3	51.3 ± 1.2	9.6 ± 0.2	2.6 ± 0.5	3.51 ± 0.12	2.99 ± 0.11	20.3 ± 0.2	16.3 ± 1.3	0.81 ± 0.06	5.22 ± 0.21	19.4 ± 0.8
90073	0.76 ± 0.08	16.9 ± 0.4	55.4 ± 1.3	8.6 ± 0.2	2.5 ± 0.4	3.09 ± 0.07	2.70 ± 0.10	20.6 ± 0.3	19.6 ± 1.6	0.95 ± 0.08	5.95 ± 0.19	22.5 ± 1.0
90152	0.26 ± 0.10	17.6 ± 0.3	58.9 ± 1.7	7.3 ± 0.1	2.8 ± 0.4	3.50 ± 0.07	2.99 ± 0.20	20.7 ± 0.4	20.5 ± 1.6	0.99 ± 0.08	5.47 ± 0.15	21.4 ± 1.6
FRO 90174 shower												
8403	–	16.2 ± 0.3	46.0 ± 1.4	5.7 ± 0.2	2.6 ± 0.3	3.72 ± 0.11	2.58 ± 0.09	17.1 ± 1.5	–	–	4.78 ± 0.17	19.7 ± 0.9
90012	–	20.1 ± 0.5	59.5 ± 1.7	8.7 ± 0.2	4.6 ± 0.4	3.57 ± 0.09	2.37 ± 0.07	15.8 ± 0.2	9.6 ± 2.1	0.61 ± 0.13	6.24 ± 0.23	27.7 ± 1.1
90087	–	18.8 ± 0.3	60.5 ± 2.0	9.2 ± 0.2	8.0 ± 0.5	3.18 ± 0.08	2.25 ± 0.10	14.2 ± 0.2	9.9 ± 1.4	0.70 ± 0.10	6.46 ± 0.18	29.5 ± 1.6
90107	–	18.2 ± 0.2	52.6 ± 1.3	7.3 ± 0.2	5.0 ± 0.7	3.78 ± 0.15	2.73 ± 0.16	14.9 ± 0.2	7.2 ± 1.8	0.48 ± 0.12	5.22 ± 0.22	21.0 ± 1.3
90174	–	17.2 ± 0.3	53.2 ± 1.8	6.7 ± 0.2	3.2 ± 0.4	3.50 ± 0.07	2.61 ± 0.09	14.9 ± 0.2	8.7 ± 1.0	0.58 ± 0.07	5.28 ± 0.14	21.9 ± 1.0
90203	–	17.5 ± 0.3	59.3 ± 2.0	13.0 ± 0.2	10.8 ± 0.5	2.61 ± 0.06	1.87 ± 0.07	12.5 ± 0.2	6.7 ± 0.8	0.54 ± 0.07	7.41 ± 0.21	35.3 ± 1.8
90204	–	18.1 ± 0.2	53.9 ± 1.6	14.2 ± 0.3	6.7 ± 0.6	2.93 ± 0.06	2.27 ± 0.12	13.9 ± 0.2	7.7 ± 3.1	0.55 ± 0.22	6.87 ± 0.17	26.7 ± 1.6
90207	–	18.1 ± 0.7	55.8 ± 1.4	18.7 ± 0.4	10.6 ± 0.8	2.60 ± 0.06	1.88 ± 0.06	12.2 ± 0.1	11.4 ± 1.5	0.93 ± 0.12	7.50 ± 0.31	32.0 ± 1.3
90211	–	18.5 ± 0.6	55.5 ± 1.3	26.2 ± 0.5	9.5 ± 0.8	2.83 ± 0.06	2.00 ± 0.09	13.0 ± 0.2	8.7 ± 0.7	0.67 ± 0.05	7.11 ± 0.29	30.3 ± 1.5
Other FRO samples												
90002	0.22 ± 0.10	17.6 ± 0.4	61.3 ± 1.8	6.8 ± 0.1	3.9 ± 0.4	4.11 ± 0.13	3.22 ± 0.19	19.9 ± 0.2	–	–	4.41 ± 0.17	19.5 ± 1.3
90043	–	19.1 ± 0.3	65.0 ± 1.9	7.6 ± 0.1	3.6 ± 0.5	3.66 ± 0.08	2.97 ± 0.09	18.9 ± 0.2	–	–	5.36 ± 0.15	22.2 ± 0.9
90069	1.21 ± 0.01	19.8 ± 0.8	55.0 ± 1.6	6.2 ± 0.2	4.1 ± 0.3	5.11 ± 0.11	3.80 ± 0.14	23.7 ± 0.2	–	–	4.00 ± 0.17	14.8 ± 0.7
90150	1.43 ± 0.01	18.4 ± 0.3	52.7 ± 1.7	6.4 ± 0.2	3.5 ± 0.8	5.41 ± 0.27	4.08 ± 0.16	23.0 ± 0.3	–	–	3.65 ± 0.19	13.9 ± 0.7
90025	–	14.0 ± 0.2	45.4 ± 2.0	4.7 ± 0.2	2.5 ± 0.3	5.14 ± 0.13	3.55 ± 0.11	18.3 ± 0.3	10.5 ± 0.9	0.57 ± 0.05	2.88 ± 0.09	13.5 ± 0.7
90151	–	13.8 ± 0.2	37.1 ± 0.9	4.0 ± 0.2	1.1 ± 0.5	4.97 ± 0.15	3.74 ± 0.11	18.1 ± 0.4	9.2 ± 1.2	0.51 ± 0.07	2.85 ± 0.09	10.2 ± 0.4
90024	–	14.6 ± 0.2	35.1 ± 0.8	3.2 ± 0.1	0.4 ± 0.3	4.23 ± 0.10	3.14 ± 0.19	14.1 ± 0.3	4.6 ± 0.5	0.32 ± 0.04	3.75 ± 0.10	12.3 ± 0.8
90037	0.21 ± 0.03	14.7 ± 0.2	37.4 ± 1.2	4.2 ± 0.1	2.3 ± 0.3	6.09 ± 0.37	3.80 ± 0.12	19.4 ± 0.2	12.4 ± 1.1	0.64 ± 0.06	2.59 ± 0.16	10.7 ± 0.5
90048	0.54 ± 0.09	15.2 ± 0.2	61.8 ± 1.8	5.1 ± 0.1	–	5.86 ± 0.12	3.83 ± 0.11	20.8 ± 0.7	17.2 ± 0.8	0.83 ± 0.05	2.75 ± 0.08	17.2 ± 0.7
90059	0.34 ± 0.03	17.0 ± 0.3	58.6 ± 1.7	6.5 ± 0.2	3.1 ± 0.3	4.15 ± 0.09	3.16 ± 0.16	19.6 ± 0.2	14.3 ± 1.0	0.73 ± 0.05	4.17 ± 0.11	18.5 ± 1.1
90072	–	19.3 ± 0.3	49.1 ± 1.2	5.8 ± 0.1	–	5.66 ± 0.13	4.07 ± 0.15	22.9 ± 0.3	–	–	3.53 ± 0.10	12.3 ± 0.6
90082	–	15.4 ± 0.2	37.1 ± 1.5	5.0 ± 0.1	–	5.77 ± 0.12	3.52 ± 0.16	17.3 ± 0.3	8.9 ± 0.9	0.51 ± 0.06	2.96 ± 0.09	11.8 ± 0.7
90104	1.87 ± 0.09	14.3 ± 0.2	45.4 ± 1.0	7.0 ± 0.2	4.0 ± 1.3	4.29 ± 0.16	3.68 ± 0.11	23.2 ± 0.2	23.4 ± 2.6	1.01 ± 0.11	3.61 ± 0.15	13.6 ± 0.5
8401(L6)	10.4 ± 1.2	18.2 ± 0.7	52.4 ± 1.7	6.7 ± 0.2	3.7 ± 0.3	6.04 ± 0.15	4.20 ± 0.13	23.1 ± 0.4	–	–	3.02 ± 0.15	12.4 ± 0.6

Radionuclide concentrations are given in dpm/kg, errors are 1σ.

*^{10}Be, ^{26}Al and ^{36}Cl results in metal fraction are from Welten *et al.* (1999a).

†Corrected for dilution (D) of ^{10}Be(stone) and ^{26}Al(stone) in the stone fraction with oxidized metal according to $D = (1 - fM_{OX}) + 0.65 \times fM_{OX}/R$(sto/met).

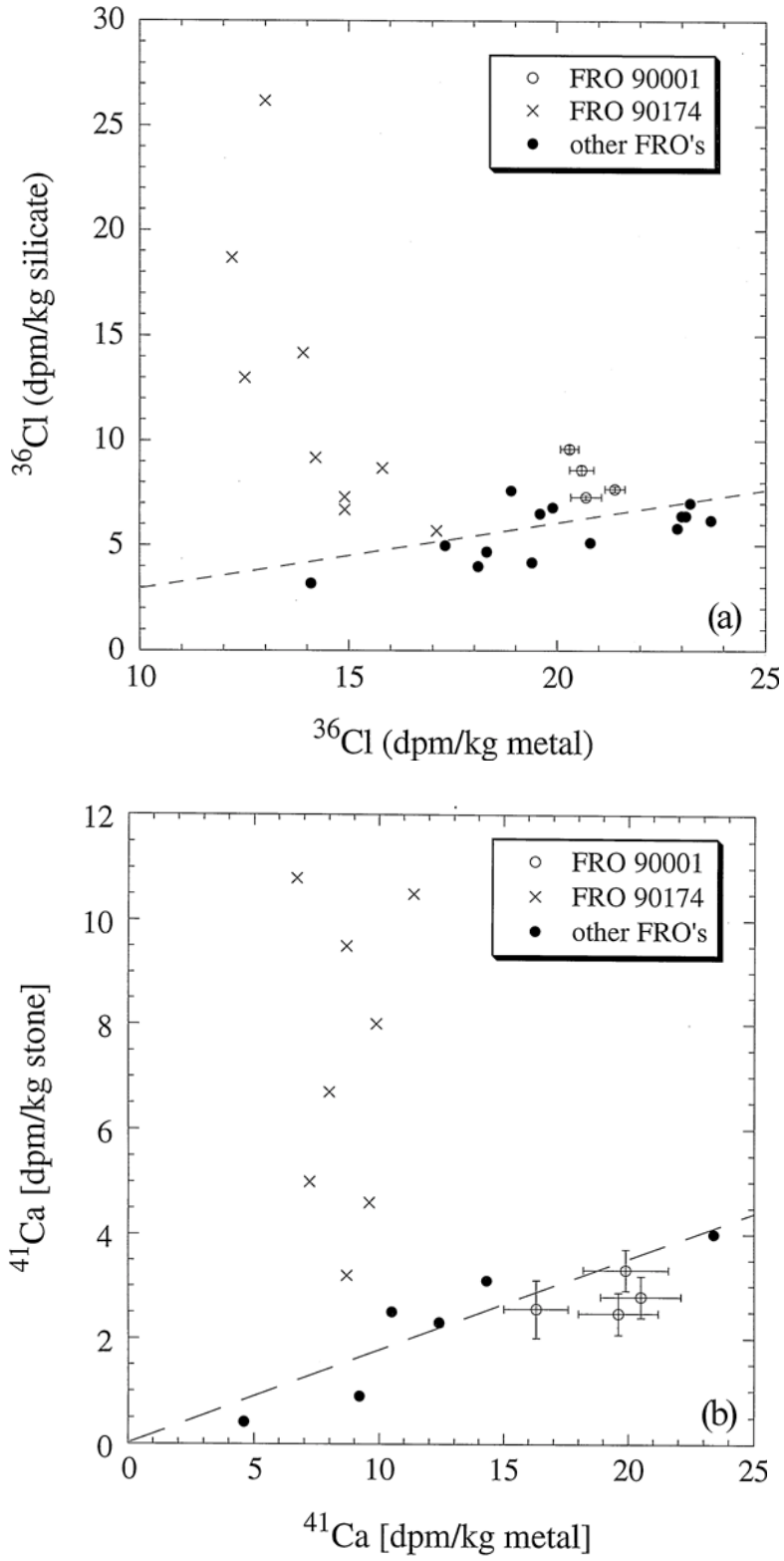

FIG. 1. Measured concentrations of ^{36}Cl (a) and ^{41}Ca (b) in the metal and silicate phase of Frontier Mountain meteorite samples. For members of the FRO 90001 shower, typical analytical uncertainties (1σ) are shown. The dotted line represents a rough estimate of the contribution of spallation produced ^{36}Cl and ^{41}Ca in the silicate phase as a function of their concentrations in the metal phase.

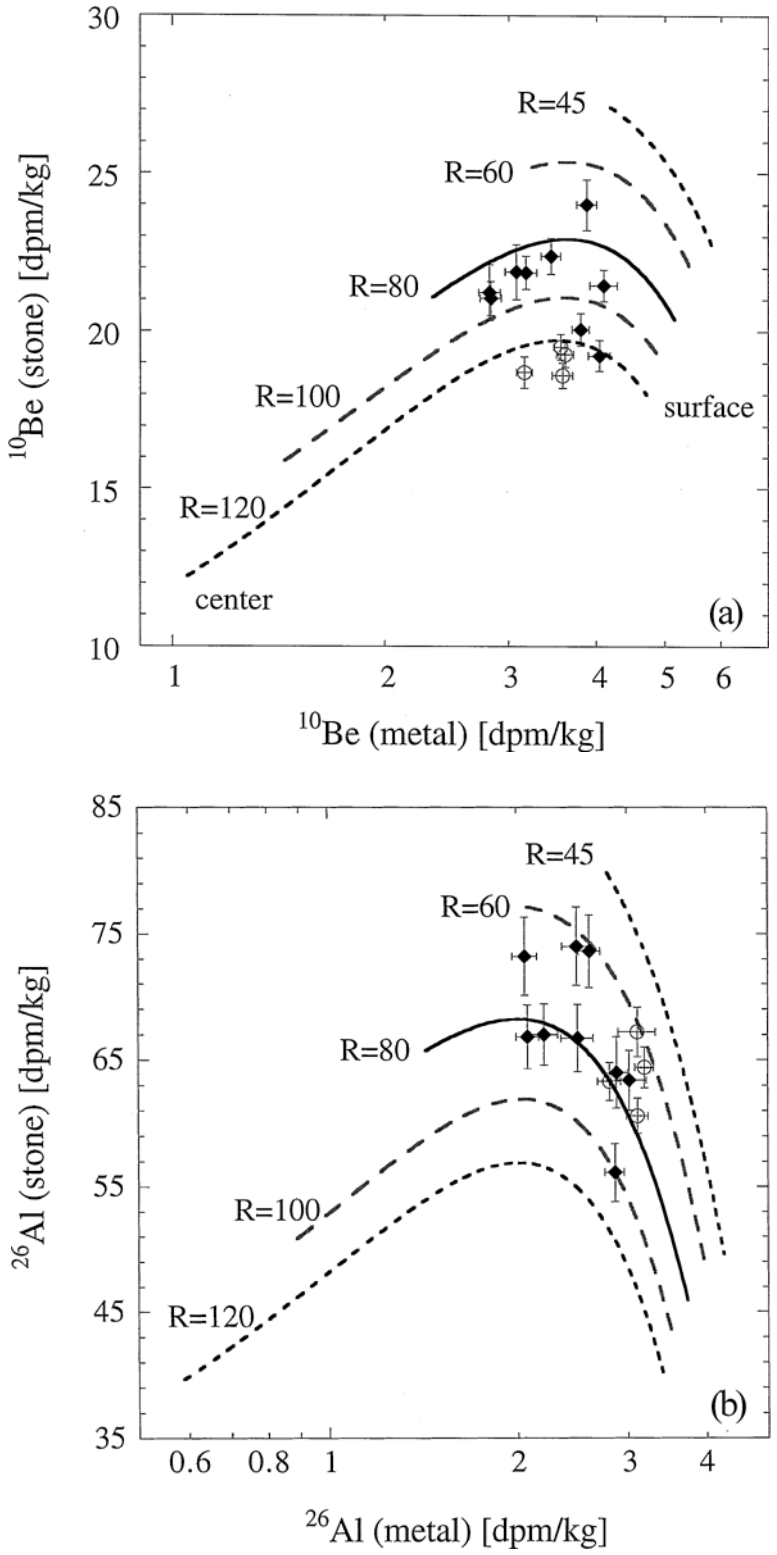

FIG. 2. Concentrations of ^{10}Be (a) and ^{26}Al (b) in stone and metal phase of the FRO 90001 (open circles) and FRO 90174 (filled circles) showers in comparison with LCS calculations for H-chondrites with radii between 45 and 120 cm. The ^{10}Be and ^{26}Al data of the FRO 900174 shower are consistent with a pre-atmospheric radius of 80–100 cm, whereas the ^{10}Be data of the FRO 90001 shower indicate a pre-atmospheric radius >120 cm for the first irradiation stage.

TABLE 3. Terrestrial ages of of Frontier Mountain H-chondrites, based on new ^{14}C and ^{41}Ca data.

Sample	*T*(terr) ^{14}C-^{10}Be	*T*(terr) ^{41}Ca-^{36}Cl	*T*(terr) ^{36}Cl-^{10}Be	*T*(terr)
FRO 90001 shower				
90001	>32	30 ± 47	(<0)	40 ± 10
90050	>44	62 ± 45	(<0)	40 ± 10
90073	>34	25 ± 47	(<0)	40 ± 10
90152	>43	16 ± 46	(<0)	40 ± 10
FRO 90174 shower				
8403	–	–	65 ± 64	100 ± 30
90012	–	125 ± 101	78 ± 39	100 ± 30
90087	–	94 ± 68	88 ± 38	100 ± 30
90107	–	179 ± 116	125 ± 42	100 ± 30
90174	–	134 ± 58	99 ± 38	100 ± 30
90203	–	155 ± 59	69 ± 34	100 ± 30
90204	–	–	64 ± 38	100 ± 30
90207	–	30 ± 66	69 ± 35	100 ± 30
90211	–	104 ± 46	84 ± 38	100 ± 30
Other FRO samples				
90002	>43	–	35 ± 48	45 ± 15
90043	–	–	26 ± 46	45 ± 15
90069	32 ± 2	–	<30	30 ± 5
90150	30 ± 2	–	13 ± 46	30 ± 5
90025	–	139 ± 49	127 ± 53	140 ± 30
90151	–	165 ± 66	133 ± 58	140 ± 30
90024	–	268 ± 61	195 ± 42	230 ± 40
90037	>42	114 ± 47	103 ± 49	110 ± 30
90048	>34	56 ± 36	64 ± 39	60 ± 30
90059	>40	86 ± 37	60 ± 51	80 ± 30
90072	–	–	17 ± 37	17 ± 37
90082	–	165 ± 55	147 ± 36	155 ± 35
90104	27 ± 2	11 ± 58	(<0)	27 ± 2
8401	13 ± 2	–	19 ± 37	13 ± 2

Terrestrial ages are given in ka. Errors in the ^{41}Ca-^{36}Cl ages include 2σ-uncertainties of radionuclide analyses as well as a 12% uncertainty in the ^{41}Ca/^{36}Cl production rate (1.06 ± 0.13). The ^{36}Cl-^{10}Be ages of members of the FRO 90174 shower and of FRO 90207 were recalculated using exposure ages of 7.2 and 10.5 Ma, respectively (Table 6). Negative ^{36}Cl-^{10}Be ages are shown in parentheses, since they are due to complex exposure histories.

the situation is more complicated due to its complex exposure history. The high ^{36}Cl saturation activities of 22–24 dpm/kg in the metal phase indicate a pre-atmospheric radius of ≤30 cm during the last ~1 Ma. However, the ^{26}Al data seem to indicate a radius of 60–80 cm, whereas the ^{10}Be data indicate a radius of >120 cm. The ^{10}Be data are most likely to reflect the shielding conditions of the first-stage exposure, which apparently occurred in a very large object. Based on these data alone we can not exclude that the first stage involved 2π-irradiation on the surface of the H-chondrite parent-body, followed by a 4π-irradiation in a medium-sized object. However, with a maximum saturation value of ~12 dpm/kg under 2π-irradiation (Graf *et al*., 1990; Leya *et al*., 2000), the second stage must have lasted at least 1.5 Ma in order to obtain ^{10}Be concentrations of ~19 dpm/kg in the stone fraction. The neutron-capture produced ^{36}Cl and ^{41}Ca should further constrain the exposure history of the two showers as well as the depth of each sample in the meteoroids.

Spallation Corrections

The production of ^{36}Cl and ^{41}Ca in the silicate phase is a mixture of spallation and thermal neutron-capture. In order to isolate the thermal neutron-capture component, the spallation component in the silicate phase was estimated on the basis of the measured ^{36}Cl and ^{41}Ca concentrations in the metal phase and the concentrations of major target elements (Fe, Ni, Ca and K) in the silicate phase. The contribution of spallation-produced ^{41}Ca in the silicate phase can easily be calculated (Table 4), since it is directly proportional to the concentration of ^{41}Ca in the metal phase and the concentrations of Fe + Ni in the silicate phase. The contribution of spallation-produced ^{36}Cl in the silicate phase cannot be determined as accurately, because the contributions from Ca and K are highly shielding dependent and have to be estimated relative to the spallation contribution from Fe. Empirical production rate ratios are $P(^{36}Cl)_{Ca}/P(^{36}Cl)_{Fe} = 8$ and $P(^{36}Cl)_{K}/P(^{36}Cl)_{Ca} = 4$ (Begemann *et al*., 1976). However, our LCS calculations show that the ^{36}Cl production rate ratio is not constant, but increases from ~4 in small objects to ~25 in the center of H-chondrites with a radius of 200 cm (Fig. 3). The LCS calculations also show that the contribution of K is constant relative to Ca, but with an average $P(^{36}Cl)_{K}/P(^{36}Cl)_{Ca}$ ratio of 1.8 ± 0.2 instead of 4. Calculated $P(^{36}Cl)_{Ca}/P(^{36}Cl)_{Fe}$ ratios in the outer 20 cm of a large H-chondrite increase from 9 to 15, which agrees with the ratio of 12 derived from lunar surface cores at depths between 25 and 75 g/cm^2 (Nishiizumi *et al*., 1991b). In addition, the LCS calculations show a good correlation ($R = 0.998$) between the $P(^{36}Cl)_{Ca}/P(^{36}Cl)_{Fe}$ ratio and the ^{10}Be(stone)/^{10}Be(metal) ratio, an empirical shielding parameter recently discussed by Welten *et al.* (1999c).

$$\frac{P(^{36}\mathrm{Cl})_{\mathrm{Ca}}}{P(^{36}\mathrm{Cl})_{\mathrm{Fe}}} = 27.6 \times \log\left(\frac{^{10}\mathrm{Be(stone)}}{^{10}\mathrm{Be(metal)}}\right) - 7.3 \qquad (2)$$

This correlation can be used to calculate the spallation contribution of ^{36}Cl from Ca, since the concentration of ^{10}Be was measured in both the stone and metal phase (Table 2). The calculated $P(^{36}Cl)_{Ca}/P(^{36}Cl)_{Fe}$ ratios for the FRO meteorites measured in this work range from 4.1 for FRO 90037 to values of 16–17 for the three most shielded members of the FRO 90174 shower (Table 4). Due to the complex exposure history of the FRO 90001 shower, the ^{10}Be(stone)/^{10}Be(metal) ratio is not a reliable shielding indicator for the last ~1 Ma. We adopted $P(^{36}Cl)_{Ca}/P(^{36}Cl)_{Fe}$ ratios of 10 ± 2 for the four members of the FRO 90001 shower, assuming a pre-atmospheric radius of ≤30 cm which is based on the high ^{36}Cl concentrations in the metal phase.

TABLE 4. Spallation and neutron-capture components of ^{36}Cl and ^{41}Ca in stone fraction of Frontier Mountain H-chondrites.

FRO	$P(^{36}Cl)_{Ca}/P(^{36}Cl)_{Fe}$*	^{36}Cl (spall)	^{41}Ca (spall)	$P(^{36}Cl)$(n-capt) at/kg min	$P(^{41}Ca)$ (n-capt) at/kg min	$P(^{41}Ca)$ (n-capt) dpm/g Ca
FRO 90001 shower						
90001	10	6.9 ± 0.6	3.3 ± 0.5	0.9 ± 0.9	<0.2	<0.02
90050	10	6.8 ± 0.5	3.4 ± 0.6	3.1 ± 0.9	≤0	≤0
90073	10	6.6 ± 0.6	3.2 ± 0.5	2.2 ± 0.9	≤0	≤0
90152	10	6.7 ± 0.6	3.2 ± 0.5	0.7 ± 0.9	≤0	≤0
FRO 90174 shower						
8403	11.4	6.1 ± 0.7	2.2 ± 0.4	–0.5 ± 1.5	0.3 ± 0.6	0.05 ± 0.09
90012	14.6	6.2 ± 0.6	1.8 ± 0.4	3.2 ± 0.9	4.9 ± 1.0	0.39 ± 0.08
90087	15.0	5.7 ± 0.5	1.8 ± 0.2	4.4 ± 0.8	10.8 ± 1.1	0.96 ± 0.09
90107	12.4	5.3 ± 0.5	1.2 ± 0.3	2.5 ± 0.8	6.4 ± 1.3	0.51 ± 0.08
90174	12.6	5.3 ± 0.5	1.5 ± 0.2	1.7 ± 0.8	2.9 ± 0.8	0.25 ± 0.07
90203	16.7	5.3 ± 0.5	1.2 ± 0.1	9.7 ± 1.0	16.5 ± 1.3	1.52 ± 0.09
90204	15.8	6.0 ± 0.5	1.5 ± 0.6	10.3 ± 1.1	9.0 ± 1.4	0.77 ± 0.12
90207	16.8	5.3 ± 0.5	1.9 ± 0.3	16.9 ± 1.3	14.9 ± 1.4	1.23 ± 0.12
90211	16.2	5.3 ± 0.5	1.5 ± 0.1	26.4 ± 1.8	13.8 ± 1.4	1.26 ± 0.13
Other FRO samples						
90002	10.5	6.5 ± 0.5	2.6 ± 0.3	0.4 ± 0.8	1.5 ± 0.8	0.10 ± 0.05
90043	12.8	6.7 ± 0.5	2.4 ± 0.3	1.0 ± 0.8	1.3 ± 0.8	0.09 ± 0.05
90069	9.3	7.2 ± 0.6	3.2 ± 0.4	–1.1 ± 0.9	0.4 ± 0.6	0.03 ± 0.04
90150	8.2	6.8 ± 0.6	3.7 ± 0.5	–0.5 ± 0.8	≤0	≤0
90025	5.4	4.7 ± 0.4	1.7 ± 0.2	0.0 ± 0.8	1.7 ± 0.8	0.11 ± 0.05
90151	5.2	4.2 ± 0.5	1.3 ± 0.2	–0.3 ± 0.7	≤0	≤0
90024	4.0	3.4 ± 0.4	1.1 ± 0.2	–0.4 ± 0.6	≤0	≤0
90037	4.0	4.7 ± 0.4	2.1 ± 0.2	–0.6 ± 0.7	0.1 ± 0.7	0.01 ± 0.05
90048	4.9	5.2 ± 0.5	–	–0.1 ± 0.5	–	–
90059	9.8	5.9 ± 0.5	2.0 ± 0.3	0.6 ± 0.8	1.8 ± 0.5	0.12 ± 0.04
90072	7.8	6.6 ± 0.6	–	–0.8 ± 0.8	–	–
90082	5.7	5.0 ± 0.5	–	0.0 ± 0.8	–	–
90104	8.0	6.9 ± 0.6	4.0 ± 0.4	0.1 ± 0.8	–0.1 ± 1.0	≤0.10
8401	6.0	5.8 ± 0.6	3.7 ± 0.3	0.6 ± 0.7	0.0 ± 0.6	≤0.04

Neutron-capture produced components of ^{36}Cl and ^{41}Ca were calculated on the basis of measured concentrations in the silicate fraction, corrected for spallation contributions (in dpm/kg) on Fe and Ni (for ^{41}Ca) and on Fe, Ni, Ca and K (for ^{36}Cl).
*Calculated using the correlation $P(^{36}Cl)_{Ca}/P(^{36}Cl)_{Fe} = 27.6 \times \log(^{10}Be_{sto}/^{10}Be_{met}) - 7.3$. All neutron-capture results were calculated after terrestrial age correction.

Neutron-Capture ^{36}Cl and ^{41}Ca Activities

The contributions of neutron-capture ^{36}Cl and ^{41}Ca are determined by subtracting spallation components from total ^{36}Cl and ^{41}Ca activities in the silicate phase (Table 4). For most FRO samples the excesses of ^{36}Cl and/or ^{41}Ca are not significant or very small, except for the members of the FRO 90174 shower, which show large contributions of neutron-capture ^{36}Cl and ^{41}Ca. The neutron-capture saturation activities in the FRO 90174 shower are up to 27 dpm/kg stone for ^{36}Cl and up to ~19 dpm/kg stone for ^{41}Ca (Table 4). These high neutron-capture activities corroborate a large pre-atmospheric size of this shower.

Figure 4 shows that the neutron-capture produced ^{36}Cl in the stone fraction of the FRO 90174 shower is inversely correlated to spallation-produced ^{36}Cl in the metal phase. Except for the high ^{36}Cl neutron-capture component in FRO 90211, the experimental results are consistent with calculated values for a wide range of shielding depths in H-chondrites with a pre-atmospheric radius of 60–100 cm and a bulk Cl concentration of 80 ppm. The production rate of neutron-capture ^{36}Cl is relative to the concentration of intrinsic Cl, which may vary considerably from meteorite to meteorite and from sample to sample within a meteorite (Garrison *et al*., 2000). Unfortunately, the concentration of intrinsic Cl is difficult to determine for Antarctic meteorites due to terrestrial

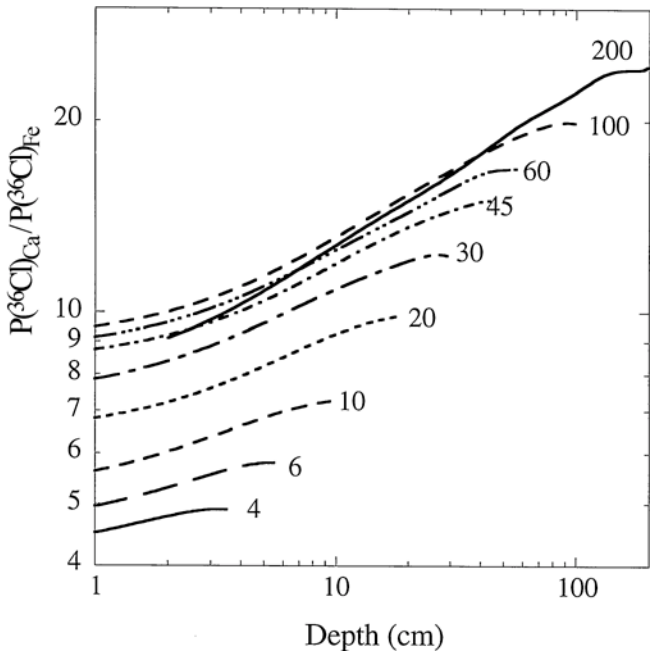

FIG. 3. Elemental production rate of ^{36}Cl from Ca relative to that from Fe, as a function of size and depth, based on LCS calculations for H-chondrites with radii of 4–200 cm.

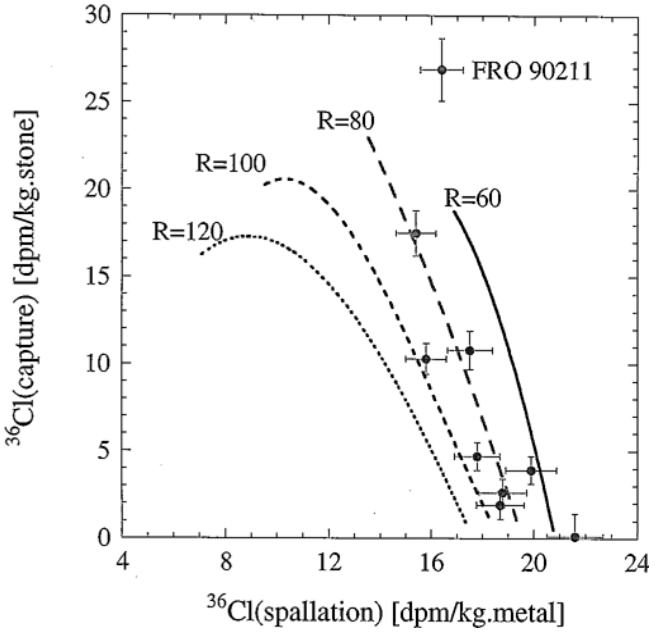

FIG. 4. Neutron-capture produced ^{36}Cl in the silicate phase and spallation-produced ^{36}Cl in the metal phase of the FRO 90174 shower, compared to LCS model calculations for H-chondrites with radii of 60–120 cm and bulk Cl contents of 80 ppm.

contamination (Langenauer and Krähenbühl, 1993). In addition, it was argued that the formation of Fe-Ni corrosion products such as akaganéite may have redistributed some of the intrinsic and terrestrial Cl (and possibly also cosmogenic ^{36}Cl) within weathered Antarctic chondrites (Buchwald and

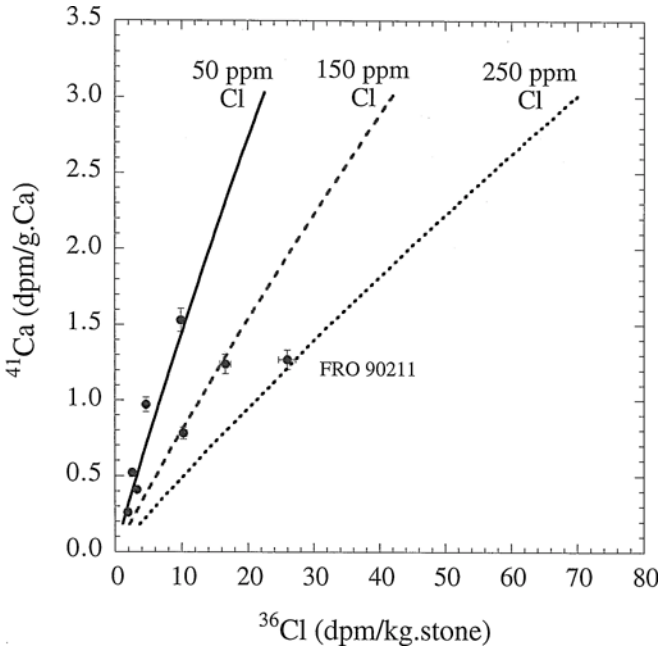

FIG. 5. Neutron-capture produced ^{36}Cl and ^{41}Ca in the silicate fraction of the FRO 90174 shower, compared to LCS model calculations for H-chondrites (asumming 1.25% Ca) with radii of 100 cm and with Cl contents increasing from 50 to 250 ppm.

Clarke, 1989). It is therefore extremely difficult to obtain the specific activity (per g Cl) of neutron-capture ^{36}Cl in Antarctic meteorite samples. On the other hand, the intrinsic concentration of Ca is relatively constant, easy to measure and much less sensitive to terrestrial contamination. The neutron-capture component of ^{41}Ca is therefore a more reliable indicator of thermal neutron fluxes in Antarctic meteorites than the neutron-capture ^{36}Cl component. In fact, Fig. 5 suggests that some of the high ^{36}Cl values (FRO 90204, 90207, 90211) are mainly due to high intrinsic Cl concentrations of 150–250 ppm rather than to high neutron-fluxes in the center of a large object.

The maximum neutron-capture component of ^{41}Ca, measured in FRO 90203, corresponds to ~1.5 dpm/g Ca. This value is higher than the maximum values measured in the Apollo 15 core (1.05 dpm/g Ca) and Allende (1.25 dpm/g Ca), comparable to Chico (1.53 dpm/g Ca), but lower than in Jilin (2.0 dpm/g Ca) (Nishiizumi *et al*., 1997b, 1991a; Klein *et al*., 1991; Bogard *et al*., 1995). Figure 6a shows the neutron-capture ^{41}Ca production rates calculated by LCS for H-chondrites with radii of 60–120 cm. The neutron-capture ^{41}Ca concentrations up to 1.5 dpm/g Ca correspond to a maximum shielding depth of 25 cm. This is supported by the maximum ^{10}Be(stone)/^{10}Be(metal) and ^{26}Al(stone)/^{26}Al(metal) ratios, which indicate a maximum depth of 30–35 cm in objects with a radius ranging from 80 to 120 cm (Fig. 6b,c). The same ratios can also be found in the center of an object with a radius of 60 cm, but this would be inconsistent with the measured neutron-capture ^{41}Ca, which is much lower than the calculated values of ~2.5 dpm/g Ca. The combined data set thus constrains the pre-atmospheric

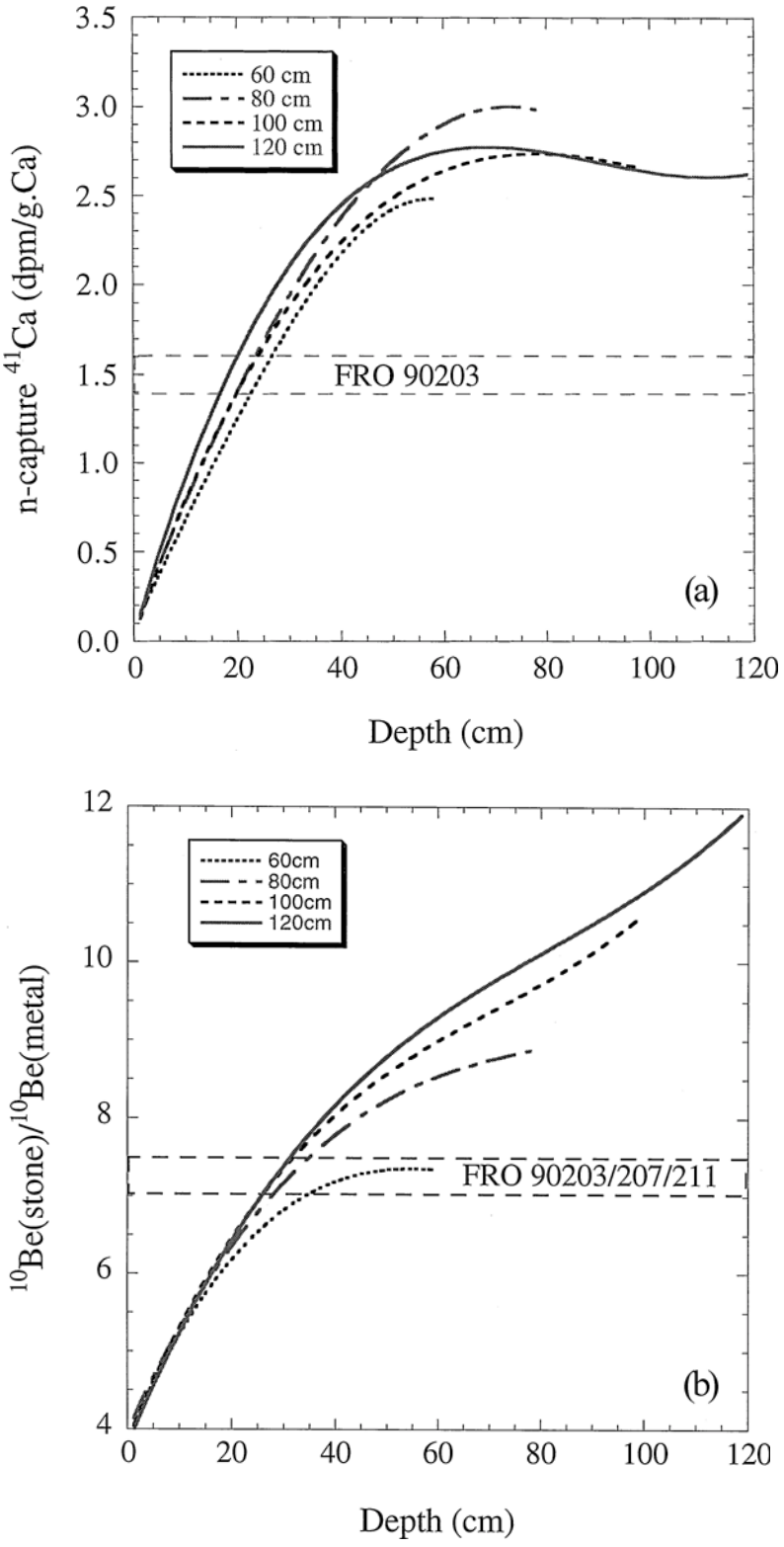

FIG. 6. Estimation of depth for samples of the FRO 90174 shower, based on neutron-capture ^{41}Ca (a) as well as on stone/metal ratios of ^{10}Be and ^{26}Al (b, above; c, overleaf). Figure (a) indicates that the neutron-capture ^{41}Ca results, normalized to dpm/g Ca, agree with sample depths of less than 25 cm in objects >60 cm in radius. The ^{10}Be and ^{26}Al results confirm sample depths of less than ~30 cm, and constrain the pre-atmospheric radius to ≥80 cm.

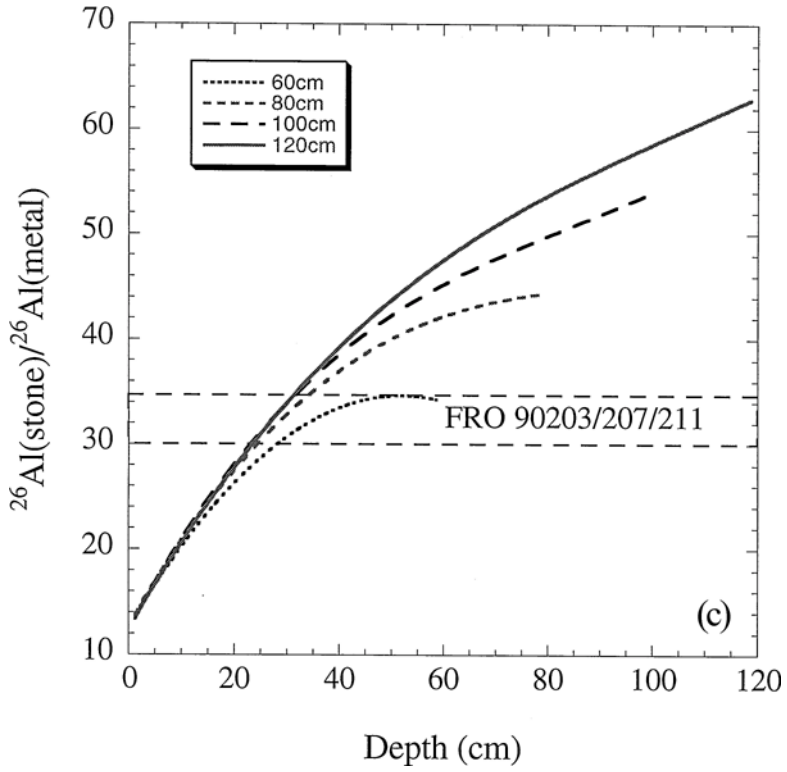

FIG. 6. *Continued.*

radius of the FRO 90174 shower to 80–100 cm. It may seem coincidental that all fragments come from the outer 30 cm, but for an object with a radius of 80–100 cm, the outer 30 cm makes up 65–75% of the total volume. It is quite possible that the interior portion of this shower survived as one (or several) large pieces, similar to the Jilin meteorite, which has a comparable pre-atmospheric radius of 85 cm (Jilin Consortium Study I, 1985).

Despite the very low ^{22}Ne/^{21}Ne ratios (1.05–1.08), the FRO 90001 shower only shows a small component (1–3 dpm/kg) of neutron-capture ^{36}Cl and no significant excess of ^{41}Ca. This is consistent with a complex exposure history with high shielding in the first and low shielding conditions in the second stage. According to this scenario, the second-stage exposure must have lasted ~1.0 Ma (*i.e.*, long enough for all neutron-capture ^{41}Ca to decay), but short enough to retain ~10% of the neutron-capture ^{36}Cl. In order to explain the high ^{10}Be in the meteorite, this relatively short second-stage irradiation excludes 2π-irradiation on the surface of the H-chondrite parent body and suggests a 4π-irradiation in an object with a large radius, most likely between 150 and 300 cm.

Neutron-Capture ^{36}Ar (From ^{36}Cl)

The measured ^{36}Ar/^{38}Ar ratios of FRO samples vary from 1.0 to 4.8, which means they are considerably higher than the cosmogenic ratio of 0.65 (Wieler *et al*., 1989). The three highest ratios (4.0–4.8) found in FRO 90002, 90012 and 90043 can be attributed to solar gases, as discussed in Welten *et al*. (1999a), but the remaining samples still show values between 1.0 and 3.9. These high ratios are mainly due to primordial Ar, but some of the samples may also contain a significant ^{36}Ar component from the decay of neutron-capture produced ^{36}Cl. If we do not correct for this neutron-capture component, then the primordial Ar component will be overestimated, which results in an over-correction for ^{38}Ar and thus to an underestimation of the ^{38}Ar exposure age. In fact, Table 5 shows that without corrections for neutron-capture ^{36}Ar, the ^{38}Ar exposure ages are up to 30% lower than the ^{21}Ne ages for the FRO 90174 shower, and up to 50% lower for the FRO 90001 shower.

From the measured concentrations of neutron-capture ^{36}Cl in the silicate fraction of shower FRO 90174 and an exposure age of 7.2 Ma, as will be explained in the next section, we calculated concentrations of neutron-capture ^{36}Ar in the range of $\sim 5 \times 10^{-10}$ cm^3 STP/g for the least shielded samples to $\sim 3.6 \times 10^{-9}$ cm^3 STP/g for the most shielded samples (Table 5). The effect of these values on the cosmogenic ^{38}Ar concentration is only 3–5% for FRO 90012, 90087, 90107 and 90174, but ranges from 10–30% for FRO 90203, 90204, 90207 and 90211. For the FRO 90001 shower, the contribution of neutron-capture ^{36}Ar is more difficult to estimate because of its complex exposure history. Assuming

TABLE 5. Contribution of ^{36}Ar from neutron-capture produced ^{36}Cl and corrected cosmogenic ^{38}Ar concentrations in members of Frontier Mountain H-chondrite showers.

FRO	^{36}Ar (meas)*	^{38}Ar (meas)*	^{38}Ar (cos-1)	$T(^{38}Ar)/T(^{21}Ne)$	^{36}Cl (n-capt)	^{36}Ar (n-capt)	^{38}Ar (cos-2)	$T(^{38}Ar)/T(^{21}Ne)$
FRO 90001 shower								
90001	0.52	0.25	0.17 ± 0.01	0.85	9 ± 9	0.12 ± 0.11	0.20 ± 0.03	0.98
90050	0.91	0.25	0.09 ± 0.01	0.48	31 ± 9	0.43 ± 0.11	0.18 ± 0.03	0.97
90073	0.43	0.21	0.15 ± 0.01	0.81	22 ± 9	0.29 ± 0.12	0.21 ± 0.03	1.15
90152	0.39	0.24	0.19 ± 0.01	0.92	7 ± 9	0.09 ± 0.11	0.21 ± 0.03	1.01
FRO 90174 shower								
8403	0.84	0.34	0.21 ± 0.01	1.00	–0.5 ± 1.5	<0.01	0.21 ± 0.01	1.00
90012	4.65	1.16	0.33 ± 0.03	(1.22)	3.2 ± 0.9	0.04 ± 0.01	0.34 ± 0.05	(1.25)
90087	0.67	0.32	0.22 ± 0.01	0.94	4.4 ± 0.9	0.06 ± 0.01	0.24 ± 0.01	1.00
90107	2.78	0.72	0.23 ± 0.02	0.98	2.5 ± 0.8	0.03 ± 0.01	0.23 ± 0.03	1.01
90174	0.93	0.35	0.20 ± 0.01	0.85	1.7 ± 0.8	0.02 ± 0.01	0.21 ± 0.01	0.87
90203	0.70	0.31	0.20 ± 0.01	0.85	9.7 ± 1.0	0.13 ± 0.02	0.23 ± 0.01	0.97
90204	0.64	0.28	0.18 ± 0.01	0.83	10.3 ± 1.1	0.14 ± 0.02	0.21 ± 0.01	0.96
90211	1.33	0.39	0.16 ± 0.01	0.69	26.4 ± 1.8	0.35 ± 0.03	0.24 ± 0.02	1.02
(90207)	0.91	0.41	0.27 ± 0.01	0.86	16.9 ± 1.3	0.33 ± 0.03	0.34 ± 0.02	1.08

*Noble gas concentrations (in 10^{-8} cm^3 STP/g) from Welten *et al.* (1999a), uncertainties in measured Ar concentrations are ~5%. The concentration of cosmogenic ^{38}Ar, before (cos-1) and after (cos-2) correction for neutron-capture ^{36}Ar, was calculated assuming ^{36}Ar/^{38}Ar ratios of 5.32 for the trapped component and of 0.65 for the cosmogenic component (Eugster, 1988). The ^{21}Ne and ^{38}Ar exposure ages were calculated using the production rates of Eugster (1988), but with a 13% lower production rate for ^{38}Ar (Schultz *et al.*, 1991). Saturation activities for neutron-capture ^{36}Cl are given in dpm/kg. Neutron-capture produced ^{36}Ar was calculated on the basis of a two-stage exposure history for the FRO 90001 shower, with a total exposure of 8 Ma and a second-stage exposure of 1.0 Ma (see text). For members of the FRO 90174 shower, we adopted a simple exposure history of 7.2 Ma, except for FRO 90207 which may represent a separate fall with an exposure age of 10.5 Ma. The cosmogenic ^{38}Ar concentrations and thus the $T(^{38}Ar)/T(^{21}Ne)$ ratios of FRO 90012 have large uncertainties due to the high contribution of solar Ar.

that the second stage lasted ~1 Ma and no neutron-capture ^{36}Cl was formed in the second stage, we find cosmogenic ^{38}Ar concentrations up to a factor of 2 higher than without corrections for neutron-capture ^{36}Ar (Table 5). After corrections for neutron-capture ^{36}Ar, the ^{38}Ar exposure ages agree within 10% with the ^{21}Ne ages for both showers (Table 5).

Exposure Ages Based on ^{10}Be-^{21}Ne and ^{26}Al-^{21}Ne Pairs

Previous suggestions that the ^{22}Ne/^{21}Ne ratio is not a reliable shielding parameter under high shielding conditions have recently been supported by model calculations which show that the ^{21}Ne production rate obtained from the "Bern-line" is overestimated for ^{22}Ne/^{21}Ne ratios <1.09 (Graf *et al.*, 1990; Leya *et al.*, 2000; Masarik *et al.*, 2000). In our previous paper (Welten *et al.*, 1999a) we calculated ^{21}Ne production rates for samples with low ^{22}Ne/^{21}Ne ratios according to the model of Graf *et al.* (1990), assuming meteoroid radii of 40–60 cm. Since the radius of the FRO 90174 meteorite shower is now estimated to be 80–100 cm, the ^{21}Ne production rates in these samples are probably 30–40% lower than previously assumed and we thus significantly underestimated the cosmic-ray exposure age of this meteorite, which was reported to be 5.5 ± 1.1 Ma (Welten *et al.*, 1999a). For the FRO 90001 shower, the situation is little more complicated due to its complex exposure history. However, most of the cosmogenic ^{21}Ne was formed during the first stage in an object >150 cm in radius. Therefore, we probably also underestimated the ^{21}Ne exposure age for the FRO 90001 shower, which showed an average age of 6.4 ± 1.7 Ma, but for which we adopted an age of 4.5 ± 0.9 Ma, based on the ^{21}Ne age of the least shielded sample (Welten *et al.*, 1999a).

The model of Graf *et al.* (1990) proposes to use ^{10}Be and ^{26}Al as internal shielding parameters to calculate ^{21}Ne production rates. The $P(^{10}Be)/P(^{21}Ne)$ and $P(^{26}Al)/P(^{21}Ne)$ ratios are relatively independent of shielding and their correlation with the ^{22}Ne/^{21}Ne ratio has been experimentally determined for objects with radii between 15 and 45 cm. The model of Graf *et al.* (1990) reproduces the experimental results and extrapolates the calculations to larger objects. We calculated the exposure age of the FRO 90174 and the FRO 90001 H-chondrite showers using the measured ^{10}Be/^{21}Ne and ^{26}Al/^{21}Ne ratios and the model parameters in Table 3 of Graf *et al.* (1990). First, we calculated the bulk ^{10}Be and ^{26}Al

contents (in at/g) at the time of fall from the measured ^{10}Be and ^{26}Al concentrations in the metal and silicate fractions and the terrestrial age (Table 6). After converting the ^{21}Ne concentrations to units of at/g, we calculated the exposure ages on the basis of Eqs. (3) and (4), shown below, and the $P(^{10}\text{Be})/P(^{21}\text{Ne})$ and $P(^{26}\text{Al})/P(^{21}\text{Ne})$ ratios (in at/at) given by Graf *et al.* (1990).

$$\frac{^{10}\text{Be}}{^{21}\text{Ne}} = \frac{P(^{10}\text{Be})}{P(^{21}\text{Ne})} \times \frac{(1-e^{-\lambda(^{10}\text{Be})\times T_{\text{exp}}})}{\lambda(^{10}\text{Be})\times T_{\text{exp}}} \quad (3)$$

$$\frac{^{26}\text{Al}}{^{21}\text{Ne}} = \frac{P(^{26}\text{Al})}{P(^{21}\text{Ne})} \times \frac{(1-e^{-\lambda(^{26}\text{Al})\times T_{\text{exp}}})}{\lambda(^{26}\text{Al})\times T_{\text{exp}}} \quad (4)$$

Eight of the nine members of the FRO 90174 shower show ^{10}Be/^{21}Ne and ^{26}Al/^{21}Ne ages in a narrow range of 6.5–8.1 Ma (Table 6), with averages of 7.3 ± 0.5 and 7.1 ± 0.4 Ma, respectively. Only FRO 90207 shows a significantly higher age (10.6 ± 0.7 Ma) as a result of its ~40% higher ^{21}Ne concentration. Since FRO 90207 also shows 30–40% higher cosmogenic ^{3}He and ^{38}Ar concentrations, it is doubtful that this meteorite is part of the FRO 90174 shower. Interestingly, the revised exposure age of the FRO 90174 shower now overlaps with the major H-chondrite peak at 7–8 Ma.

The exposure age of the FRO 90174 shower corresponds to ^{21}Ne production rates of $(0.22–0.30) \times 10^{-8}$ cm^3 STP/g Ma. These values are consistent with ^{21}Ne production rates of $(0.22–0.29) \times 10^{-8}$ cm^3 STP/g Ma which follow from our LCS model calculations for an object with a radius of 80–100 cm. However, we remind the reader that more care has to be taken for very small meteoroids, say with ^{22}Ne/^{21}Ne ratios of >1.20 (Welten *et al*., 1994). This is confirmed by Table 6, which shows that for low-shielding samples the ^{10}Be/^{21}Ne and ^{26}Al/^{21}Ne ages are up to 40% and 60% lower than the corresponding ^{21}Ne ages based on the formalism of Eugster (1988), which has proven to be reliable for low shielding conditions. The large discrepancies of the ^{26}Al/^{21}Ne ages of FRO 90025, 90037 and 90048 are believed to be an artifact of the contribution of solar-cosmic-ray produced ^{26}Al in the stone fraction, which leads to an overestimation of the ^{21}Ne production rate. However, the low ^{10}Be/^{21}Ne ages of FRO 90151, 90025 and 90037 are demonstrating that the nearly constant ^{10}Be/^{21}Ne ratio proposed by Graf *et al*. (1990) is not valid for very low shielding conditions. Interestingly enough, the ^{10}Be/^{21}Ne and ^{26}Al/^{21}Ne ages of FRO 90072 and 90082 are closer to the main H-chondrite peak at 7–8 Ma than the previously reported ^{21}Ne ages of 8.2 and 9.1 Ma (Welten *et al*., 1999a).

The four members of the FRO 90001 shower show ^{10}Be/^{21}Ne and ^{26}Al/^{21}Ne ages between 6.5 and 7.7 Ma, with an average of 7.3 ± 0.5 and 7.0 ± 0.4 Ma, respectively (Table 6). However, Eqs. (3) and (4) underestimate the exposure age in the case of a complex exposure history such as FRO 90001, since the radionuclide concentrations adjust faster to the higher production rates of the second stage than the ^{21}Ne concentration. Using reasonable production rates for both irradiation stages, we arrive at a total exposure age between 7 and 9 Ma. The revised exposure ages of the two H-chondrite showers now coincide with the main H-chondrite peak at 7–8 Ma, thereby reinforcing the existence of a peak which was previously barely visible in the exposure age distribution of FRO H-chondrites (Welten *et al*., 1999a). About half of the H-chondrites we studied belong to the 7–8 Ma peak; non-Antarctic meteorites display a similar distribution.

H/L-Chondrite Ratio at Frontier Mountain

Previously we discussed the role of large H-chondrite showers in explaining the high H- to L-chondrite ratio (3.0) at Frontier Mountain (Welten *et al*., 1999a). Here we confirm that the FRO 90001 and FRO 90174 showers play a significant role, since together they represent 50% of the 26 randomly selected H5/H6 chondrite samples. In addition, the large pre-atmospheric size of the FRO 90174 shower makes it likely that about a third of all H5/H6 chondrites in the Frontier Mountain collection belong to this single shower. If we assume that the two showers represent half of all H-chondrites at Frontier Mountain, the H-/L-chondrite ratio would be reduced from the observed value of 3.0 to ~1.5, which is close to the ratio of ~1.0 for non-Antarctic falls. However, this ratio does not take into account that the collection of L-chondrites from Frontier Mountain, which has not been studied in such detail yet, possibly also contains one or several showers. Therefore, we conclude that the two H-chondrite showers partly explain the high H-/L-chondrite ratio at Frontier Mountain, but that other factors such as a higher occurrence of fragmentation among H-chondrites, probably also play a significant role (Welten *et al*., 1999a).

CONCLUSIONS

The determination of neutron-capture ^{36}Cl and ^{41}Ca in the silicate phase of two Frontier Mountain H-chondrite showers, in addition to spallation-produced radionuclides, provides a wealth of information about the cosmic-ray exposure history of these two objects: (1) The measured concentrations of ^{36}Cl and ^{41}Ca in the silicate phase of the FRO 90174 shower, corrected for a terrestrial age of 100 ka give neutron-capture production rates up to ~27 atoms/min/kg for ^{36}Cl and ~19 atoms/min/kg for ^{41}Ca. According to our theoretical model calculations, the concentrations of spallation-produced ^{10}Be and ^{26}Al as well as neutron-capture produced ^{36}Cl and ^{41}Ca are consistent with those in the outer 25–35 cm of an object with a pre-atmospheric radius of 80–100 cm. This suggests that the FRO 90174 shower represents one of the largest pre-atmospheric size chondrites in Antarctica. It is possible that more-shielded samples of the FRO 90174 meteoroid will be found among other H5/6

TABLE 6. Shielding corrected $^{10}Be/^{21}Ne$ and $^{26}Al/^{21}Ne$ cosmic-ray exposure ages of the two FRO H-chondrite showers and of samples with low shielding, based on $^{22}Ne/^{21}Ne$ ratios ≥1.20.

FRO	$^{21}Ne^*$	$^{22}Ne/^{21}Ne^*$	^{10}Be bulk	^{26}Al bulk	$^{10}Be/^{21}Ne$ at/at	$^{26}Al/^{21}Ne$ at/at	$P(^{10}Be)/P(^{21}Ne)$	$P(^{26}Al)/P(^{21}Ne)$	T_{exp*} (^{21}Ne)	T_{exp} $^{10}Be/^{21}Ne$	T_{exp} $^{26}Al/^{21}Ne$
FRO 90001 shower											
90001	1.75	1.06	15.8 ± 0.4	51.1 ± 2.0	0.038 ± 0.002	0.058 ± 0.004	0.139	0.423	6.1	7.6 ± 0.5	7.4 ± 0.5
90050	1.52	1.075	15.6 ± 0.6	49.4 ± 2.2	0.044 ± 0.003	0.065 ± 0.004	0.139	0.413	4.5	6.6 ± 0.5	6.5 ± 0.5
90073	1.64	1.05	15.5 ± 0.5	51.0 ± 2.2	0.040 ± 0.002	0.062 ± 0.004	0.138	0.430	8.6	7.2 ± 0.5	7.0 ± 0.5
90152	1.78	1.06	15.8 ± 0.4	52.8 ± 3.8	0.038 ± 0.002	0.059 ± 0.005	0.139	0.423	6.4	7.7 ± 0.5	7.3 ± 0.7
FRO 90174 shower											
8403	1.58	1.09	15.3 ± 0.5	44.7 ± 2.1	0.041 ± 0.003	0.056 ± 0.004	0.140	0.401	4.7	7.1 ± 0.5	7.2 ± 0.5
90012	2.12	1.08	19.3 ± 0.7	59.0 ± 2.4	0.038 ± 0.002	0.055 ± 0.004	0.140	0.410	6.9	7.6 ± 0.5	7.5 ± 0.5
90087	1.93	1.07	18.0 ± 0.6	60.4 ± 3.3	0.040 ± 0.002	0.062 ± 0.005	0.139	0.416	5.9	7.3 ± 0.5	6.8 ± 0.6
90107	1.70	1.10	17.8 ± 0.7	53.2 ± 3.4	0.044 ± 0.003	0.062 ± 0.005	0.141	0.397	5.3	6.5 ± 0.5	6.5 ± 0.6
90174	1.80	1.09	16.3 ± 0.4	51.9 ± 2.5	0.038 ± 0.002	0.057 ± 0.004	0.140	0.401	5.6	7.6 ± 0.5	7.3 ± 0.6
90203	1.96	1.07	16.8 ± 0.5	59.5 ± 3.0	0.036 ± 0.002	0.060 ± 0.004	0.139	0.416	6.0	8.1 ± 0.5	7.1 ± 0.5
90204	1.81	1.07	17.6 ± 0.4	54.6 ± 3.3	0.041 ± 0.002	0.060 ± 0.005	0.139	0.416	5.5	7.0 ± 0.4	7.0 ± 0.6
90207	2.61	1.07	16.8 ± 0.7	53.5 ± 2.1	0.027 ± 0.002	0.041 ± 0.003	0.139	0.416	7.9	10.9 ± 0.8	10.4 ± 0.7
90211	1.90	1.07	17.1 ± 0.7	52.9 ± 2.6	0.038 ± 0.003	0.055 ± 0.004	0.139	0.416	5.8	7.7 ± 0.5	7.6 ± 0.6
Low shielding samples											
90072	1.84	1.20	17.2 ± 0.5	41.8 ± 1.9	0.040 ± 0.002	0.045 ± 0.003	0.146	0.331	8.2	7.7 ± 0.5	7.4 ± 0.6
90082	1.89	1.22	15.5 ± 0.4	38.4 ± 2.4	0.040 ± 0.002	0.047 ± 0.004	0.147	0.317	9.1	7.7 ± 0.5	6.9 ± 0.7
90048	6.06	1.24	14.3 ± 0.3	56.5 ± 2.8	0.010 ± 0.001	0.019 ± 0.001	0.148	0.304	31.1	31.9 ± 2.0	*16.7 ± 1.3*
90151	0.58	1.27	13.3 ± 0.4	37.0 ± 1.4	0.098 ± 0.006	0.128 ± 0.008	0.149	0.284	3.2	1.9 ± 0.1	1.9 ± 0.1
90025	0.66	1.28	14.1 ± 0.4	48.0 ± 2.6	0.090 ± 0.005	0.145 ± 0.011	0.150	0.278	3.8	2.5 ± 0.2	*1.5 ± 0.1*
90037	1.05	1.32	14.4 ± 0.9	37.3 ± 1.7	0.058 ± 0.005	0.071 ± 0.005	0.152	0.251	6.6	5.0 ± 0.5	*3.5 ± 0.3*

Concentrations of cosmogenic ^{21}Ne are given in (10^{-8} cm^3 STP/g), radionuclide concentrations after correction for terrestrial age in (dpm/kg bulk). Uncertainties (1σ) in ^{21}Ne concentrations are ~5%, uncertainties of the cosmogenic $^{22}Ne/^{21}Ne$ ratio are ~1%. The concentration and production ratios of $^{10}Be/^{21}Ne$, $^{26}Al/^{21}Ne$ are given in (atoms/atoms). The $^{10}Be/^{21}Ne$ and $^{26}Al/^{21}Ne$ exposure ages (Ma) are calculated on the basis of Eqs. (3) and (4) and compared to the ^{21}Ne exposure ages given by Welten *et al.* (1999a). The relatively low $^{26}Al/^{21}Ne$ exposure ages of FRO 90048, 90025 and 90037, printed in italics, are probably an artifact of the contribution of solar-cosmic-ray produced ^{26}Al in the stone fraction (Welten *et al.*, 1999c) and should therefore be disregarded.

*Data from Welten *et al.* (1999a).

chondrites in the FRO collection, unless the interior portion of the meteoroid survived as one or several large pieces, outside of the catchment area of the Frontier Mountain stranding area.

(2) A second shower (FRO 90001) containing four members shows small contributions of neutron-capture ^{36}Cl in the silicate phase, but no significant component of neutron-capture ^{41}Ca. We propose a complex exposure history in which the low ^{22}Ne/^{21}Ne ratios and the small neutron-capture component of ^{36}Cl are a relict of high shielding during the first stage, followed by lower shielding conditions during a second stage, which started ~1.0 Ma ago. This meteoroid with a radius of 150–300 cm was produced at the 7–8 Ma H-chondrite collisional event and broke up again 1.0 Ma ago, delivering a small to medium sized object (R < 30 cm) to Earth. This scenario is consistent with recently developed models of meteorite delivery from the asteroid belt to Earth, which propose that the Yarkovsky orbital drift slowly transports meter-sized meteoroids from the main belt to the resonances, after which the meteoroids are perturbed into Earth-crossing orbits within a few million years (Farinella and Vokrouhlicky, 1999; Hartmann *et al.*, 1999).

(3) On the basis of measured ^{10}Be/^{21}Ne and ^{26}Al/^{21}Ne ratios and semi-empirical ratios from the model of Graf *et al.* (1990), we revise the cosmic-ray exposure ages of the FRO 90174 and FRO 90001 showers to 7.2 ± 0.5 Ma and 8 ± 1 Ma, respectively. These ages coincide with the well-established peak for H-chondrites at 7–8 Ma.

(4) We corrected for the neutron-capture component of ^{36}Ar based on measured neutron-capture ^{36}Cl and obtained better agreement between the cosmogenic ^{21}Ne and ^{38}Ar exposure ages for members of the two showers.

(5) The new radionuclide data confirm the two pairing groups and suggest that 8 of the 26 H5/6-chondrites (31%) belong to the FRO 90174 shower. Combined with the large pre-atmospheric size of the FRO 90174 meteoroid, it is quite possible that 25–50% of all H5/6 chondrites at Frontier Mountain belong to this single shower. This large shower partially explains the high H- to L-chondrite ratio at Frontier Mountain.

Acknowledgments–We wish to thank EUROMET, especially Arabelle Sexton and Ludolf Schultz, for providing the meteorite samples. Don DePaolo at Lawrence Berkeley National Laboratory graciously made space available for sample processing. The paper greatly benefited from reviews by Phil Bland, Eric Gilabert and the Associate Editor, Ian Lyon. This work was supported by NASA grants NAG5-4832 and NAG5-4992, N. S. F. grant OPP-9316272, the Swiss National Science Foundation, LLL-UCDRD, and was performed under the auspices of the U.S. D. O. E. by L.L.N.L. under contract W-7405-ENG-48.

Editorial handling: I. C. Lyon

REFERENCES

BEGEMANN F., WEBER H. W., VILCSEK E. AND HINTENBERGER H. (1976) Rare gases and ^{36}Cl in stony-iron meteorites: Cosmogenic elemental production rates, exposure ages, diffusion losses and thermal histories. *Geochim. Cosmochim. Acta* **40**, 353–368.

BOGARD D. D., NYQUIST L. E., BANSAL B. M., GARRISON D. H., WIESMANN H., HERZOG G. F. ALBRECHT A. A., VOGT S. AND KLEIN J. (1995) Neutron-capture ^{36}Cl, ^{41}Ca, ^{36}Ar and ^{150}Sm in large chondrites: Evidence for high fluences of thermalized neutrons. *J. Geophys. Res.* **100**, 9401–9416.

BOTTKE W. F., RUBINCAM D. P AND BURNS J. A. (2000) Dynamical evolution of main belt asteroids: Numerical simulations incorporating planetary perturbations and Yarkovsky thermal forces. *Icarus* **145**, 301–331.

BRIESMEISTER J. F. (1993) *MCNP—A General Monte Carlo N-Particle Transport Code, Version 4A.* Los Alamos Natioal Laboratory report LA-12625-M, Los Alamos, New Mexico, USA. 693 pp.

BUCHWALD V. F. AND CLARKE R. S., JR. (1989) Corrosion of Fe-Ni aloys by Cl-containing akaganéite (β-FeOOH): The Antarctic meteorite case. *Am. Mineral.* **74**, 656–667.

CRESSY P. J., JR. (1972) Cosmogenic radionuclides in the Allende and Murchison carbonaceous chondrites. *J. Geophys. Res.* **77**, 4905–4911.

DAVIS J. C. *ET AL.* (1990) LLNL/UC AMS facility and research program. *Nucl. Instrum. Methods* **B52**, 269–272.

EUGSTER O. (1988) Cosmic-ray production rates of ^{3}He, ^{21}Ne, ^{38}Ar, ^{83}Kr and ^{126}Xe in chondrites based on ^{81}Kr-Kr exposure ages. *Geochim. Cosmochim. Acta* **52**, 1649–1662.

FARINELLA P. AND VOKROUHLICKY D. (1999) Semimajor axis mobility of asteroidal fragments. *Science* **283**, 1507–1510.

GARRISON D., HAMLIN S. AND BOGARD D. (2000) Chlorine abundances in meteorites. *Meteorit. Planet. Sci.* **35**, 419–429.

GRAF T., BAUR H. AND SIGNER P. (1990) A model for the production of cosmogenic nuclides in chondrites. *Geochim. Cosmochim. Acta* **54**, 2521–2534.

HARTMANN W. K., FARINELLA P., VOKROUHLICKY D., WEIDENSCHILLING S. J., MORBIDELLI A., MARZARI F., DAVIS D. R. AND RYAN E. (1999) Reviewing the Yarkovsky effect: New light on the delivery of stone and iron meteorites from the asteroid belt (abstract). *Meteorit. Planet. Sci.* **34 (Suppl.)**, A161–A167.

HERZOG G. F., VOGT S., ALBRECHT A., XUE S., FINK D., KLEIN J., MIDDLETON R., WEBER H. W. AND SCHULTZ L. (1997) Complex exposure histories for meteorites with "short" exposure ages. *Meteorit. Planet. Sci.* **32**, 413–422.

HUSS G. R. (1991) Meteorite mass distributions and differences between Antarctic and non-Antarctic meteorites. *Geochim. Cosmochim. Acta* **55**, 105–111.

JAROSEWICH E. (1990) Chemical analyses of meteorites: A compilation of stony and iron meteorites. *Meteoritics* **25**, 323–337.

JILIN CONSORTIUM STUDY I (1985) Eight papers on the Jilin meteorite. *Earth Planet. Sci. Lett.* **72**, 246–310.

JULL A. J. T., S. CLOUDT S. AND CIELASZYK E. (1998) ^{14}C terrestrial ages of meteorites from Victoria Land, Antarctica and the infall rate of meteorites. In *Meteorites: Flux with Time and Impact Effects* (eds. G. J. McCall, R. Hutchison, M. M. Grady and D. Rothery), pp. 75–91. Geological Society of London Special Publication 140, London, U.K.

JULL A. J. T., BLAND P., KLANDRUD S. E., MCHARGUE L. R., BEVAN A. W. R., KRING D. AND WLOTZKA F. (2000) Using ^{14}C and ^{14}C-^{10}Be for terrestrial ages of desert meteorites. In *Workshop on Extraterrestrial Materials from Cold and Hot Deserts* (eds. L. Schultz, I. Franchi, A. Reid and M. Zolensky), pp. 41–43. LPI Contribution No. 997, Lunar and Planetary Institute, Houston, Texas, USA.

KLEIN J., FINK D., MIDDLETON R., VOGT S. AND HERZOG G. F. (1991) ^{41}Ca in the Jilin (H5) chondrite: A matter of size (abstract). *Meteoritics* **26**, 358.

KÖNIG H., KEIL K., HINTENBERGER H., WLOTZKA F. AND BEGEMANN F. (1961) Untersuchungen an Steinmeteoriten mit extrem hohem Edelgasgehalt, I. *Der Chondrit Pantar. Z. Naturf.* **16a**, 1124–1130.

LANGENAUER M. AND KRÄHENBÜHL U. (1993) Halogen contamination in Antarctic H5 and H6 chondrites and relation to sites of recovery. *Earth Planet. Sci. Lett.* **120**, 431–442.

LEYA I., LANGE H-J., NEUMANN S., WIELER R. AND MICHEL R. (2000) The production of cosmogenic nuclides in stony meteoroids by galactic cosmic-ray particles. *Meteorit. Planet. Sci.* **35**, 259–286.

MASARIK J. AND REEDY R. C. (1994) Effects of bulk composition on nuclear production processes in meteorites. *Geochim. Cosmochim. Acta* **58**, 5307–5317.

MASARIK J., NISHIIZUMI K. AND REEDY R. C. (2000) Simulation of cosmogenic noble gas production in ordinary chondrites and the lunar surface (abstract). *Meteorit. Planet. Sci.* **35 (Suppl.)**, A104.

MASON B. (1979) Cosmochemistry Part I. Meteorites. In *Data of Geochemistry* (ed. M. Fleischer). Geological Survey Professional Paper 440-B-1. U.S. Govt. Printing Office, Washington, D.C., USA. 132 pp.

MORBIDELLI A. AND GLADMAN B. (1998) Orbital and temporal distributions of meteorites originating in the asteroid belt. *Meteorit. Planet. Sci.* **33**, 999–1016.

MUGHABGHAB S. F., DIVADEENAM M. AND HOLDEN N. E. (1981) Neutron resonance parameters and thermal cross sections, Part A, Z = 1–60. In *Neutron Cross Sections 1*, Academic Press, New York, New York, USA.

NISHIIZUMI K. AND CAFFEE M. W. (1998) Measurements of cosmogenic ^{41}Ca and ^{41}Ca/^{36}Cl terrestrial ages (abstract). *Meteorit. Planet. Sci.* **33 (Suppl.)**, A117.

NISHIIZUMI K., ELMORE D., MA X. Z. AND ARNOLD J. R. (1984) ^{10}Be and ^{26}Al depth profiles in an Apollo 15 drill core. *Earth Planet. Sci. Lett.* **70**, 157–163.

NISHIIZUMI K., ARNOLD J. R., FINK D., KLEIN J. AND MIDDLETON R. (1991a) ^{41}Ca Production profile in the Allende meteorite (abstract). *Meteoritics* **26**, 379.

NISHIIZUMI K., ARNOLD J. R., SHARMA P., KUBIK P. W. AND REEDY R. C. (1991b) Cosmogenic ^{36}Cl production rate on the lunar surface (abstract). *Lunar Planet. Sci.* **22**, 979–980.

NISHIIZUMI K., CAFFEE M. W., JEANNOT J-P., LAVIELLE B. AND HONDA M. (1997a) A systematic study of the cosmic-ray exposure history of iron meteorites: Beryllium-10-chlorine-36/beryllium-10 terrestrial ages (abstract). *Meteorit. Planet. Sci.* **32 (Suppl.)**, A100.

NISHIIZUMI K., FINK D., KLEIN J., MIDDLETON R., MASARIK J., REEDY R. C. AND ARNOLD J. R. (1997b) Depth profile of ^{41}Ca in an Apollo 15 drill core and the low-energy neutron flux in the Moon. *Earth Planet. Sci. Lett.* **148**, 545–552.

NISHIIZUMI K., CAFFEE M. W. AND DEPAOLO D. J. (2000) Preparation of a ^{41}Ca AMS standards. *Nucl. Instrum. Methods B* **172**, 399–403.

PRAEL R.E. AND LICHTENSTEIN H. (1989) *User Guide to LCS: The LAHET Code System*. Los Alamos National Laboratory report, LA-UR-89-3014, Los Alamos, New Mexico, USA. 76 pp.

RAMBALDI E. R., CENDALES M. AND THACKER R. (1978) Trace element distribution between magnetic and non-magnetic portions of ordinary chondrites. *Earth Planet. Sci. Lett.* **40**, 175–186.

REEDY R. C., MASARIK J., NISHIIZUMI K., ARNOLD J. R., FINKEL R. C., CAFFEE M. W., SOUTHON J., JULL A. J. T. AND DONAHUE D. J. (1993) Cosmogenic radionuclide profiles in Knyahinya: New measurements and models (abstract). *Lunar Planet. Sci.* **24**, 1195–1196.

SCHULTZ L., WEBER H. W. AND BEGEMANN F. (1991) Noble gases in H-chondrites and potential differences between Antarctic and non-Antarctic meteorites. *Geochim. Cosmochim. Acta* **55**, 59–66.

SHARMA P., KUBIK P. W., FEHN U., GOVE G. E., NISHIIZUMI K. AND ELMORE D. (1990) Development of ^{36}Cl standards for AMS. *Nucl. Instrum. Methods* **B52**, 410–415.

VOGT S. K. *ET AL.* (1993) On the Bur Ghelaui H5 chondrite and other meteorites with complex exposure histories. *Meteorit. Planet. Sci.* **28**, 71–85.

WELTEN K. C. (1999) Concentrations of siderophile elements in nonmagnetic fractions of Antarctic H- and L-chondrites: A quantitative approach to weathering effects. *Meteorit. Planet. Sci.* **34**, 259–270.

WELTEN K. C. AND NISHIIZUMI K. (2000) Degree of weathering of H-chondrites from Frontier Mountain, Antarctica. In *Workshop on Extraterrestrial Materials from Cold and Hot Deserts* (eds. L. Schultz, I. Franchi, A. Reid and M. Zolensky), pp. 83–87. LPI Contribution No. 997, Lunar and Planetary Institute, Houston, Texas, USA.

WELTEN K. C., LINDNER L., VAN DER BORG K., ALDERLIESTEN C., VAN ROIJEN J. J., DE JONG A. F. M. AND SCHULTZ L. (1994) AMS measurements of ^{10}Be and ^{26}Al for studying shielding effects in meteorites. *Nucl. Instrum. Methods* **B92**, 500–504.

WELTEN K. C., NISHIIZUMI K., CAFFEE M. W., SCHÄFER J. AND WIELER R. (1999a) Terrestrial ages and exposure ages of Antarctic H-chondrites from Frontier Mountain, North Victoria Land. *NIPR Antarct. Meteorite Res.* **12**, 94–107.

WELTEN K. C., MASARIK J., NISHIIZUMI K., CAFFEE M. W. AND WIELER R. (1999b) Neutron-capture production of ^{36}Cl and ^{41}Ca in two H-chondrite showers from Frontier Mountain, Antarctica (abstract). *Lunar Planet. Sci.* **30**, #1899, Lunar and Planetary Institute, Houston, Texas, USA (CD-ROM).

WELTEN K. C., MASARIK J., NISHIIZUMI K., CAFFEE M. W. AND WIELER R. (1999c) The stone/metal ratios of ^{10}Be and ^{26}Al as empirical shielding parameters in ordinary chondrites (abstract). *Meteorit. Planet. Sci.* **34 (Suppl.)**, A121–122.

WIELER R., GRAF T., PEDRONI A., SIGNER P., PELLAS P., FIENI C., SUTER M., VOGT S., CLAYTON R. N. AND LAUL J. C. (1989) Exposure history of the regolithic chondrite Fayetteville: II. Solar-gas-free light inclusions. *Geochim. Cosmochim. Acta* **53**, 1449–1459.

Back

Forward

Table of Contents